

# REPORT DOCUMENTATION PAGE

*Form Approved*  
*OMB No. 0704-0188*

Public reporting burden for this collection of information is estimated to average 1 hour per response, including the time for reviewing instructions, searching existing data sources, gathering and maintaining the data needed, and completing and reviewing this collection of information. Send comments regarding this burden estimate or any other aspect of this collection of information, including suggestions for reducing this burden to Department of Defense, Washington Headquarters Services, Directorate for Information Operations and Reports (0704-0188), 1215 Jefferson Davis Highway, Suite 1204, Arlington, VA 22202-4302. Respondents should be aware that notwithstanding any other provision of law, no person shall be subject to any penalty for failing to comply with a collection of information if it does not display a currently valid OMB control number. **PLEASE DO NOT RETURN YOUR FORM TO THE ABOVE ADDRESS.**

<b>1. REPORT DATE (DD-MM-YYYY)</b> 18-03-2010		<b>2. REPORT TYPE</b> Journal Article		<b>3. DATES COVERED (From - To)</b>	
<b>4. TITLE AND SUBTITLE</b>  <b>Thermal Transitions and Reaction Kinetics of Polyhedral Silsesquioxane Containing Phenylethynylphthalimides (Preprint)</b>				<b>5a. CONTRACT NUMBER</b>	
				<b>5b. GRANT NUMBER</b>	
				<b>5c. PROGRAM ELEMENT NUMBER</b>	
<b>6. AUTHOR(S)</b> Bradley Seurer & Andre Lee (Michigan State Univ.); Vandana Vij & Timothy Haddad (ERC); Joseph M. Mabry (AFRL/RZSM)				<b>5d. PROJECT NUMBER</b>	
				<b>5e. TASK NUMBER</b>	
				<b>5f. WORK UNIT NUMBER</b> 23030521	
<b>7. PERFORMING ORGANIZATION NAME(S) AND ADDRESS(ES)</b>  Air Force Research Laboratory (AFMC) AFRL/RZSM 9 Antares Road Edwards AFB CA 93524-7401				<b>8. PERFORMING ORGANIZATION REPORT NUMBER</b>  AFRL-RZ-ED-JA-2010-100	
<b>9. SPONSORING / MONITORING AGENCY NAME(S) AND ADDRESS(ES)</b>  Air Force Research Laboratory (AFMC) AFRL/RZS 5 Pollux Drive Edwards AFB CA 93524-7048				<b>10. SPONSOR/MONITOR'S ACRONYM(S)</b>	
				<b>11. SPONSOR/MONITOR'S NUMBER(S)</b> AFRL-RZ-ED-JA-2010-100	
<b>12. DISTRIBUTION / AVAILABILITY STATEMENT</b>  Approved for public release; distribution unlimited (PA #10171).					
<b>13. SUPPLEMENTARY NOTES</b> For publication in Macromolecules.					
<b>14. ABSTRACT</b>  Thermal transitions and reaction kinetics of polyhedral oligomeric silsesquioxane (POSS) with a phenylethynylphthalimide (PEPI) moiety were investigated. Specifically, this study was aimed to understand the influence of the POSS periphery, types of spacer group in between the PEPI and the SiO core, architecture of PEPI arrangement with respect to the SiO core, and number of PEPI groups per cage on the thermal transitions and the crosslinking reaction of phenylethynyl. PEPI-POSS compounds with a phenyl periphery show higher melting temperatures as compared to those with isobutyl peripheries. PEPI-POSS compounds with isobutyl peripheries show a higher phenylethynyl reaction rate than those PEPI-POSS compounds with phenyl peripheries. Changing the spacer group from propyl to phenyl increases the melting transition temperature as well as higher heat of fusion at melting; however the more rigid phenyl spacer enables the PEPI-POSS form a higher degree of crystallinity upon cooling. The more rigid phenyl spacer also initiates the polyene reactions at lower temperatures, but at higher temperatures, some reaction pathways become restricted leading to a lower overall extent of reaction.					
<b>15. SUBJECT TERMS</b>					
<b>16. SECURITY CLASSIFICATION OF:</b>			<b>17. LIMITATION OF ABSTRACT</b>	<b>18. NUMBER OF PAGES</b>	<b>19a. NAME OF RESPONSIBLE PERSON</b>
<b>a. REPORT</b>	<b>b. ABSTRACT</b>	<b>c. THIS PAGE</b>			Dr. Joseph M. Mabry
<b>Unclassified</b>	<b>Unclassified</b>	<b>Unclassified</b>	SAR	42	<b>19b. TELEPHONE NUMBER (include area code)</b> N/A

**Thermal Transitions and Reaction Kinetics of Polyhedral Silsesquioxane containing  
Phenylethynylphthalimides (Preprint)**

Bradley Seurer<sup>1</sup>, Vandana Vij<sup>2</sup>, Timothy Haddad<sup>2</sup>, Joseph M. Mabry<sup>3\*</sup>, Andre Lee<sup>1\*</sup>

<sup>1</sup>Department of Chemical Engineering & Materials Science  
Michigan State University  
East Lansing, MI 48823

<sup>2</sup>ERC, Inc.  
Air Force Research Laboratory  
RZSM, Bldg. 8451, 10 E Saturn Boulevard  
Edwards AFB, CA 93524-7680

<sup>3</sup>Air Force Research Laboratory  
RZSM, Bldg. 8451, 10 E Saturn Boulevard  
Edwards AFB, CA 93524-7680

\* To whom correspondence should be addressed

E-mail: [leea@egr.msu.edu](mailto:leea@egr.msu.edu); [Joseph.Mabry@edwards.af.mil](mailto:Joseph.Mabry@edwards.af.mil)

Distribution Statement A: Approved for public release; distribution unlimited.

## **ABSTRACT**

Thermal transitions and reaction kinetics of polyhedral oligomeric silsesquioxane (POSS) with a phenylethynylphthalimide (PEPI) moiety were investigated. Specifically, this study was aimed to understand the influence of the POSS periphery, types of spacer group in between the PEPI and the SiO core, architecture of PEPI arrangement with respect to the SiO core, and number of PEPI groups per cage on the thermal transitions and the crosslinking reaction of phenylethynyl. PEPI-POSS compounds with a phenyl periphery show higher melting temperatures as compared to those with isobutyl peripheries. PEPI-POSS compounds with isobutyl peripheries show a higher phenylethynyl reaction rate than those PEPI-POSS compounds with phenyl peripheries. Changing the spacer group from propyl to phenyl increases the melting transition temperature as well as higher heat of fusion at melting; however the more rigid phenyl spacer enables the PEPI-POSS form a higher degree of crystallinity upon cooling. The more rigid phenyl spacer also initiates the polyene reactions at lower temperatures, but at higher temperatures, some reaction pathways become restricted leading to a lower overall extent of reaction. For POSS with two PEPI groups, due to the bulky shape of “in-chain” attachment relative to the POSS core, it was more difficult to form a crystalline phase as compared to having both PEPI groups come off from the same corner. For molecules with two PEPI groups at the same corner, the overall extent reaction was the lowest among all PEPI-POSS molecules investigated. Finally, it was found that these PEPI-POSS molecules have reaction kinetics on par with organic hexafluorophenylethynyl oligoimides, which make these PEPI-POSS molecules excellent candidates for use as matrix materials in high performance composite applications.

**Keywords:** Silsesquioxanes, Phenylethynylphthalimide, Thermal transitions, Reaction kinetics

## INTRODUCTION

Chemical and physical interactions of reacting monomers can affect the kinetics of polymerization, which ultimately influence the performance of the resultant polymer. Recent advancements in the synthesis of nano-structured inorganic/organic hybrid materials with reactive moieties have prompted a surge of efforts to incorporate these hybrids into organic polymers.<sup>1-14</sup> However, the performance of these copolymers depends on the molecular arrangement between the nano-structure hybrids and the organics. Hence, a systematic study that explores the kinetics of the reactive moiety on the hybrids, as influenced by the chemical and physical characteristics of nano-structures, is needed.

Polyhedral oligomeric silsesquioxanes (POSS) are a class of inorganic-organic hybrids with reactive moieties.<sup>1-12</sup> POSS nano-structured chemicals consist of a geometrically well-defined silicon/oxygen,  $\text{SiO}_{1.5}$ , polyhedral core surrounded with chemically specified organic peripheral groups.<sup>1-13,15-21</sup> Organic peripheral groups are covalently bonded to each silicon atom, which provides POSS molecules with specific interactions to other POSS molecules or organics in the medium.<sup>17-21</sup> In addition, the relative position of reactive groups with respect to the core of POSS may also play a role during the polymerization reactions. A few examples in literature best illustrate these points. In the case of polystyrene-POSS copolymers, the POSS peripheral group was shown to affect the  $T_g$ , the modulus above  $T_g$ , and the molecular weight of the copolymers.<sup>19</sup> This is attributed to the POSS-POSS interactions as well as the solubility of styrene-POSS of different peripheral groups in resultant copolymers. In the case of POSS modified polystyrene-polybutadiene-polystyrene triblock copolymers, depending on the peripheral group of POSS used, the effect on the phase morphology and phase transition behavior differ significantly.<sup>20</sup> Hence, it is likely that other molecular variables of POSS,

including the architecture, the number of functional groups, and nature of the spacer group connecting the SiO POSS core to the functional group will additionally influence the properties of these copolymers.

Fundamentally, studying the reactivity of POSS compounds is best accomplished in bulk reaction conditions, thereby eliminating the effects of solvent and catalyst. Therefore, a thermally activated functional group with a high onset of reaction temperature is to be used, thereby minimizing the effects of crystallinity of POSS molecules. One possible candidate is the phenylethynylphthalic imide (PEPI) functional group.<sup>22-26</sup> PEPI is chemically attached to monomers via reaction of phenylethynylphthalic anhydride (PEPA) to amines. PEPI is utilized to end-cap the aromatic heterocyclic oligoimides. Upon heating, phenylethynyl undergoes crosslink reactions to form thermosets.<sup>22-33</sup> The cure reaction of PEPI has been studied using solid state carbon NMR and infrared spectroscopy. These studies suggest that PEPI reactions proceed initially by polyene reactions, followed by branching and cyclization reactions.<sup>22-27</sup> Several kinetic studies of oligoimides end-capped with PEPI and model PEPI compounds have shown first-order kinetics for the initial polyene reactions, with a C≡C conversion of under 80%.<sup>22-23</sup> The kinetics deviate when the slow, diffusion controlled cyclization and crosslinking chemistries occur. It is also recognized that the transition from chemical-controlled to diffusion-controlled reaction kinetics is influenced by the molecular weight, molecular weight distribution, molecular structure, and chain architecture of the oligoimides used. The relatively high onset of reaction temperature of phenylethynyl, i.e. above 300°C, makes PEPI an ideal candidate to study the effects of the POSS periphery and architecture on reactivity as the thermal transitions of PEPI-POSS macromers are well separated from its phenylethynyl reactions.

Based on the above rationale, this study investigated the thermal characteristics and reaction kinetics of PEPI-functionalized POSS, as influenced by the POSS periphery, PEPI-POSS spacer group, and POSS architecture. To achieve this, a series of PEPI-POSS were designed and synthesized by appropriate chemistries. The mono, di, and octafunctional PEPI-POSS molecules used in this study are shown in Figure 1.

## EXPERIMENTAL

**Materials:** The compounds 1-(3-(5-(phenylethynyl)isoindolinyl-1,3-dione)propyl)-3,5,7,9,11,13,15-isobutylpentacyclo[9.5.1.1<sup>3,9</sup>.1<sup>5,15</sup>.1<sup>7,13</sup>]octasiloxane (Ibu<sub>7</sub>propylPEPI-POSS), 1-(3-(5-(phenylethynyl)isoindolinyl-1,3-dione)phenyl)-3,5,7,9,11,13,15-isobutylpentacyclo[9.5.1.1<sup>3,9</sup>.1<sup>5,15</sup>.1<sup>7,13</sup>]octasiloxane (Ibu<sub>7</sub>phenylPEPI-POSS), 1,3,5,7,9,11,14-hepta-phenyltricyclo[7.3.3.1<sup>5,11</sup>]heptasiloxane-endo-3,7,14-triol (Ph<sub>7</sub>trisilanol-POSS), 1,3,5,7,9,11,13,15-((octa(3-(5-(phenylethynyl)isoindolinyl-1,3-dione)propyl)-pentacyclo[9.5.1.1<sup>3,9</sup>.1<sup>5,15</sup>.1<sup>7,13</sup>]octasiloxane (OctapropylPEPI-POSS), 1,3,5,7,9,11,13,15-((octa(3-(5-(phenylethynyl)isoindolinyl-1,3-dione)phenyl)-pentacyclo[9.5.1.1<sup>3,9</sup>.1<sup>5,15</sup>.1<sup>7,13</sup>]octasiloxane (OctaphenylPEPI-POSS), and tricyclo[7.3.3(3,7)]octasiloxane-5,11,14,17-tetraol-1,3,5,7,9,11,14,17-octaphenyl (Ph<sub>8</sub>tetrasilanol-POSS) were obtained from Hybrid Plastics. Solvents such as toluene, tetrahydrofuran (THF), hexane, diethylether and dimethylacetimide (DMAc) were obtained from Aldrich and purified prior to use. Magnesium turnings, (N-trimethylsilyl)<sub>2</sub>-4-bromoaniline, aniline and triethylamine were obtained from Aldrich and used as received. Phenylethynyl phthalic anhydride (PEPA) and 2,2'-bis-(3,4-dicarboxyphenyl)hexafluoropropane dianhydride (6-FDA) were obtained from Chriskev Company. Para-phenylenediamine (p-PDA) was obtained from Aldrich. Trichloromethylsilane,

from Gelest, and tetrachlorosilane, from United Chemical Technologies, were distilled prior to use. Oligoimides of  $n$  moles of 6-FDA,  $n+1$  moles of p-PDA, and 2 moles of PEPA as the end functionality, where  $n=1$  (HFPE-n-1) or 9 (HFPE-n-9), were synthesized using the PMR method.<sup>31</sup>

## Synthetic methods

**Synthesis of ((*N*-trimethylsilyl)<sub>2</sub>-aniline-4-(dichloromethylsilane))** In a drybox under a nitrogen atmosphere, a THF solution (25 mL) of (*N*-trimethylsilyl)<sub>2</sub>-4-bromoaniline (9.483 g, 30.0 mmol) was added in a drop-wise manner to a 250 mL flask containing well-stirred magnesium turnings (0.913 g, 37.6 mmol) in a few mL of THF (just enough to cover the magnesium). Prior to starting the addition, the magnesium was activated with a small crystal of I<sub>2</sub> and a drop of (*N*-trimethylsilyl)<sub>2</sub>-4-bromoaniline. The reaction was stirred for 20 hours at room temperature. This Grignard reagent was added drop-wise to a well-stirred THF solution (10 mL) of trichloromethylsilane (5.431 g, 36.3 mmol) in a 250 mL flask. After stirring for 20 hours at room temperature, the solvent was removed under vacuum. The product was extracted with hexane and filtered to remove the insolubles. The hexane was then removed under vacuum and the product isolated by vacuum distillation. Product (6.6 g, 63 % yield) was collected from 95-110°C under 60 mtorr vacuum. NMR resonances (ppm): <sup>29</sup>Si NMR δ: 18.9 (1 Si), 5.2 (2 Si). <sup>13</sup>C NMR δ: 152.15, 133.56, 129.95, 127.62, 5.80, 2.17. <sup>1</sup>H NMR δ: 7.59 (2 H's, multiplet), 7.00 (2 H's, multiplet), 1.05 (3 H's, singlet), 0.11 (18 H's, singlet).

**Synthesis of Phenyl<sub>8</sub>bisaniline-POSS (Ph<sub>8</sub>bisaniline-POSS)** Under a nitrogen atmosphere in a dry box, a solution of ((*N*-trimethylsilyl)<sub>2</sub>-aniline-4-(dichloromethylsilane)) (2.953 g, 8.42 mmol), triethylamine (1.857 g, 18.4 mmol) and THF (10 mL) was added drop-wise via an addition funnel into a well-stirred solution of Ph<sub>8</sub>tetraol-POSS (4.455 g, 4.17 mmol) and THF (40 mL) in

a 100 mL round bottom flask. The POSS solution became cloudy after the addition of a few drops of the dichloromethylsilane/triethylamine solution, indicating formation of insoluble HNEt<sub>3</sub>Cl salt. After 30 minutes of stirring, this salt was separated by filtration and the solvent was removed under vacuum. Addition of diethylether (2 mL) followed by a solution of acidified methanol (50 mL) gave a white suspension of product that was stirred at room temperature for one hour. The product (3.90 g, 70 % yield) was isolated by filtration and dried in a vacuum oven overnight at 60°C. NMR resonances (ppm): <sup>29</sup>Si NMR δ: -29.7 (4 Si), -78.2 (8 Si), -79.1 (2 Si), -79.3 (4 Si), -79.4(2 Si). <sup>13</sup>C NMR δ: 148.27, 135.13, 134.39, 134.35, 134.30, 134.22, 132.29, 131.40, 131.19, 130.98, 130.52, 130.47, 130.38, 130.24, 127.93, 127.88, 127.69, 127.52, 124.64, 114.56, -0.10. <sup>1</sup>H NMR δ: 7.8-7.1 (44 H's, overlapping multiplets), 6.6 (4 H's, doublet), 3.6 (4 H's, NH<sub>2</sub>, broad singlet), 0.58 (6 H's, CH<sub>3</sub>, singlet).

**Synthesis of *Phenyl<sub>8</sub>bis(phenylethynylphthalimide)-POSS (Ph<sub>8</sub>bisPEPI-POSS)*** Under a nitrogen atmosphere, a well-stirred solution of Ph<sub>8</sub>bisaniline-POSS (0.248 g, 0.186 mmol) and PEPA (0.095 g, 0.38 mmol) in anhydrous THF (2 mL) and anhydrous toluene (2 mL) was heated to 60°C for 2 hours, and then to 105°C for 20 hours. Most of the solvent was removed under vacuum, and the product (0.30 g, 90 % yield) was precipitated into methanol, filtered, and dried in a vacuum oven at 125°C for 24 hours. NMR resonances (ppm): <sup>29</sup>Si NMR δ: -31.2, -77.9, -78.9, -79.1, -79.3. <sup>13</sup>C NMR δ: 166.4, 166.3, 137.1, 136.1, 134.0, 133.9, 133.2, 132.0, 131.8, 131.6, 130.9, 130.5, 130.4, 130.3, 130.0, 129.2, 128.5, 127.8, 127.8, 127.7, 127.6, 126.5, 125.5, 123.7, 121.0, 94.2, 87.7, -0.4. <sup>1</sup>H NMR δ: 8.2-7.2 (64 H's, overlapping multiplets), 0.71 (6 H's).

**Synthesis of *Phenyl<sub>7</sub>monohydroxyl-POSS (Ph<sub>7</sub>OH-POSS)*** Under a nitrogen atmosphere, a solution of silicon tetrachloride (1.903 g, 11.2 mmol) and triethylamine (3.572 g, 35.3 mmol) in THF (20 mL) was added drop-wise to a well-stirred THF (70 mL) solution of Ph<sub>7</sub>trisilanol-POSS

(9.965 g, 10.7 mmol) in a 100 mL round bottom flask. After stirring overnight at room-temperature, the suspension was filtered, collecting both  $\text{Ph}_7\text{Cl-POSS}$  product and  $\text{NEt}_3\text{HCl}$  salt byproduct. After dissolving these solids in THF (5 mL) and chloroform (15 mL), the silicon-chlorine bond was hydrolyzed with water (15 mL) and dilute HCl (2 mL) over a 90 minute period. The aqueous layer was removed and extracted twice with chloroform. The combined organic layers were extracted with water, dilute HCl, water, and saturated brine and then dried with magnesium sulfate. After filtration, most of the solvent was removed under vacuum, and the product (9.37 g, 90 % yield) was precipitated into methanol, filtered, and dried at  $40^\circ\text{C}$  in a vacuum oven overnight. NMR resonances (ppm):  $^{29}\text{Si}$  NMR  $\delta$ : -77.9 (3 Si), -78.2 (3 Si), -78.3 (1 Si), -100.4 (1 Si).  $^{13}\text{C}$  NMR  $\delta$ : 134.45, 134.39, 131.11, 131.05, 130.22, 130.10, 128.11, 128.10.  $^1\text{H}$  NMR  $\delta$ : 7.87 (14 H's, multiplet), 7.51 (7 H's, multiplet), 7.45 (14 H's, multiplet), 3.9 (1 H, broad singlet).

**Synthesis of *di((N-trimethylsilyl)<sub>2</sub>-aniline)-4,4'-(chloromethylsilane)*** The Grignard reagent,  $(\text{Me}_3\text{Si})_2\text{NC}_6\text{H}_4\text{MgBr}$  was prepared exactly as previously described from 37.6 mmol of magnesium and 30 mmol of (N-trimethylsilyl)<sub>2</sub>-4-bromoaniline in THF (25 mL). This Grignard reagent was added drop-wise to a well-stirred THF solution (10 mL) of trichloromethylsilane (2.242 g, 15.0 mmol) in a 250 mL flask. After stirring overnight at room temperature, the solvent was removed under vacuum. The product was extracted with hexane and filtered under nitrogen to remove insolubles. The hexane and some lower-boiling side products were removed under vacuum up to  $150^\circ\text{C}$ . The product (5.4 g, 65 % yield), purified by a Kugel-Rohr distillation, was isolated under 10 mtorr vacuum at  $175^\circ\text{C}$ . NMR resonances (ppm):  $^{29}\text{Si}$  NMR  $\delta$ : 10.7 (1 Si), 4.8 (4 Si).  $^{13}\text{C}$  NMR  $\delta$ : 150.6, 134.5, 129.8, 129.0, 2.2, 1.5.  $^1\text{H}$  NMR  $\delta$ : 7.46 (4 H's, multiplet), 6.94 (4 H's, multiplet), 0.90 (3 H's, singlet), 0.08 (36 H's, singlet).

**Synthesis of *Ph-* and *Ibu-monosiloxymethyldianiline-POSS* (*Ibu<sub>7</sub>* or *Ph<sub>7da</sub>-POSS*)** Under a nitrogen atmosphere, a diethylether (5 mL) solution of triethylamine (0.314 g, 3.1 mmol) and di((*N*-trimethylsilyl)<sub>2</sub>-aniline)-4,4'-(chloromethylsilane) (1.701 g, 3.08 mmol) was added, dropwise, to a POSS solution of either *Ibu<sub>7</sub>*OH-POSS (2.50 g, 3.00 mmol) or *Ph<sub>7</sub>*OH-POSS (2.92 g, 3.00 mmol) dissolved in a mixture of diethylether (15 mL) and THF (2 mL), and stirred overnight at room temperature. The solution was filtered to remove HNEt<sub>3</sub>Cl, and most of the solvent was removed under vacuum. Addition of acidified methanol (50 mL) and stirring the suspension for an hour at room temperature produced the free amine. The product (~60 % yield) was isolated by filtration, and dried in a vacuum oven overnight at 60°C. NMR resonances (ppm):

***Ph<sub>7da</sub>-POSS*:** <sup>29</sup>Si NMR δ: -8.0 (1 Si), -78.1 (3 Si), -78.2 (4 Si), -109.4 (1 Si). <sup>13</sup>C NMR δ: 147.75, 135.63, 134.53, 134.41, 130.96, 130.88, 130.38, 130.32, 128.06, 127.99, 125.63, 114.57, -0.38. <sup>1</sup>H NMR δ: 7.83 (14 H's, multiplet), 7.80 (4 H's, multiplet), 7.52 (7 H's, multiplet), 7.44 (14 H's, multiplet), 6.56 (4 H's, multiplet), 3.82 (4 H's, broad singlet), 0.62 (3 H's, singlet).

***Ibu<sub>7da</sub>-POSS*:** <sup>29</sup>Si NMR δ: -9.4 (1 Si), -67.0 (3 Si), -67.9 (4 Si), -109.9 (1 Si). <sup>13</sup>C NMR δ: 147.54, 135.60, 126.39, 114.63, 25.91, 24.06, 23.97, 22.72, 22.67, 22.54, -0.32. <sup>1</sup>H NMR δ: 7.40 (4 H's, multiplet), 6.67 (4 H's, multiplet), 3.79 (4 H's, broad singlet), 1.88 (7 H's, multiplet), 0.97 (42 H's, multiplet), 0.60 (17 H's, multiplet).

**Synthesis of *Ph-* or *Ibu-monosiloxymethyldi(phenylethynylphthalimide)-POSS* (*Ibu<sub>7</sub>* or *Ph<sub>7diPEPI-POSS</sub>*)** Under a nitrogen atmosphere, a well-stirred solution of either *Ph<sub>7da</sub>-POSS* (0.250 g, 2.06 mmol) or *Ibu<sub>7da</sub>-POSS* (0.249 g, 2.36 mmol) and PEPA (2.03 equivalents) in anhydrous THF (2 mL) and anhydrous toluene (2 mL) was heated to 60°C for 2 hours, and then to 105°C for 20 hours. Most of the solvent was removed under vacuum, and the product (~90 %

yield) was precipitated into methanol, filtered, and dried in a vacuum oven at 125°C for 24 hours.

Both products show a small impurity by silicon NMR. NMR resonances (ppm): **Ph<sub>7</sub>diPEPI-**

**POSS:** <sup>29</sup>Si NMR δ: -8.7 (1 Si), -77.8 (3 Si), -78.2 (4 Si), -109.3 (1 Si).

<sup>13</sup>C NMR δ: 166.4, 166.3, 137.1, 136.3, 134.7, 134.2, 134.1, 133.0, 132.0, 131.8, 131.7, 130.8,

130.3, 130.1, 130.0, 129.8, 129.3, 128.5, 127.9, 127.8, 126.5, 125.4, 123.7, 122.0, 94.3, 87.7, -

0.9. <sup>1</sup>H NMR δ: 8.1-7.2 (59 H's), 0.61 (3 H's).

**Ibu<sub>7</sub>diPEPI-POSS:** <sup>29</sup>Si NMR δ: -10.2 (1 Si), -66.7 (3 Si), -67.8 (4 Si), -109.6 (1 Si).

<sup>13</sup>C NMR δ: 166.5, 166.4, 137.1, 136.8, 134.7, 132.9, 132.0, 131.8, 131.5, 130.3, 130.0, 129.2,

129.1, 128.5, 128.1, 126.5, 126.4, 125.4, 123.7, 123.6, 122.0, 94.2, 87.7, 25.7, 25.6, 23.8, 23.7,

22.4, 22.3, -0.9. <sup>1</sup>H NMR δ: 8.1-7.2 (24 H's), 1.9 (7 H's), 1.0 (42 H's), 0.67 (17 H's).

**Synthesis of ((*N*-trimethylsilyl)<sub>2</sub>-aniline-4-(trichlorosilane))** In a drybox, under a nitrogen

atmosphere, a THF solution (25 mL) of (N-trimethylsilyl)<sub>2</sub>-4-bromoaniline (9.496 g, 30.0 mmol)

was added in a drop-wise manner to a 250 mL flask containing well-stirred magnesium turnings

(1.14 g, 46.9 mmol) in a few mL of THF (just enough to cover the magnesium). Prior to starting

the addition, the magnesium was activated with a small crystal of I<sub>2</sub> and a drop of (N-

trimethylsilyl)<sub>2</sub>-4-bromoaniline. The reaction was stirred overnight at room temperature. This

Grignard reagent was added drop-wise to a well-stirred THF solution (10 mL) of

tetrachlorosilane (6.105 g, 35.9 mmol) in a 250 mL flask. After stirring overnight at room

temperature, the solvent was removed under vacuum. The product was extracted with hexane

and filtered to remove the insolubles. The hexane was then removed under vacuum and the

product isolated by vacuum distillation. Product (6.1 g, 55 % yield) was collected from 95-110°C

under 60 mtorr vacuum. NMR resonances (ppm): <sup>29</sup>Si NMR δ: 5.5 (2 Si), -0.8 (1 Si). <sup>13</sup>C NMR

$\delta$ : 153.87, 133.96, 130.28, 125.92, 2.39.  $^1\text{H NMR}$   $\delta$ : 7.66 (2 H's, multiplet), 7.02 (2 H's, multiplet), 0.10 (18 H's, singlet).

**Synthesis of *Phenyl-aniline-POSS (Ph<sub>7</sub>aniline-POSS)*** In a drybox, under a nitrogen atmosphere, a THF (5 mL) solution of ((N-trimethylsilyl)<sub>2</sub>-aniline-4-(trichlorosilane) (0.871 g, 2.35 mmol) and triethylamine (0.680 g, 6.72 mmol) was slowly added in a drop-wise manner to a well-stirred THF (10 mL) solution of Ph<sub>7</sub>trisilanol-POSS (2.015 g, 2.16 mmol) in a 100 mL round bottom flask. This solution became cloudy after the addition of a few drops, indicating formation of HNEt<sub>3</sub>Cl salt. After stirring at room-temperature overnight, filtration was used to separate product from salt, and the solvent was removed under vacuum. The free-amine was produced by addition of diethylether (2 mL) followed by a solution of acidified methanol (20 mL) and stirring for 1 hour at room temperature. The product (1.36 g, 60 % yield) was collected by filtration and dried in a vacuum oven overnight. NMR resonances (ppm): CD<sub>2</sub>Cl<sub>2</sub>  $^{29}\text{Si NMR}$   $\delta$ : -77.0 (1 Si), -78.3 (4 Si), -78.5 (3 Si).  $^1\text{H NMR}$   $\delta$ : 8.0-6.8 (37 H's, multiplet), 6.7 (2 H's, doublet), 3.6 (2 H's, broad singlet).

**Synthesis of *Ph<sub>7</sub>(phenylethynylphthalimide)-POSS (Ph<sub>7</sub>PEPI-POSS)*** A solution of (1.049 g, 1.00 mmol) of Ph<sub>7</sub>aniline-POSS in toluene (25 mL) and (0.250 g, 1.01 mmol) of PEPA in DMAc (3 mL) were mixed in a 100 mL round bottom flask equipped with a 20 mL Dean-Stark apparatus. The solution was heated to 110°C (oil bath at 150°C) for 5 hours. After cooling, the product (1.23 g, 95 % yield) was precipitated into methanol, filtered, and dried in a vacuum oven at 120°C for 24 hours. NMR resonances (ppm):  $^{29}\text{Si NMR}$   $\delta$ : -78.1 (3 Si), -78.2 (4 Si), -78.7 (1 Si).  $^{13}\text{C NMR}$   $\delta$ : 166.7, 166.6, 137.5, 135.3, 134.3, 134.1, 132.2, 132.1, 131.1, 131.0, 130.5, 130.5, 130.3, 130.2, 129.5, 128.8, 128.2, 128.1, 126.8, 125.8, 124.0, 122.2, 94.6, 87.9.  $^1\text{H NMR}$   $\delta$ : 8.2-6.7 (overlapping multiplets).

## Characterization

Nuclear magnetic resonance spectroscopy was performed on a Bruker 300 spectrometer, using CDCl<sub>3</sub> solvent (unless otherwise noted), for <sup>1</sup>H (300 MHz), <sup>13</sup>C (75 MHz), and <sup>29</sup>Si (60 MHz). NMR spectroscopy was also performed using a Varian Unity 500 spectrometer, for <sup>1</sup>H (500 MHz), <sup>13</sup>C (125 MHz), and <sup>29</sup>Si (99 MHz). Spectra are referenced to internal CDCl<sub>3</sub> at 7.26 ppm (<sup>1</sup>H) and 77.23 ppm (<sup>13</sup>C). <sup>29</sup>Si spectra are referenced to external Me<sub>4</sub>Si at 0 ppm. Thermal characteristics and crosslink reactions were studied using Differential scanning calorimetry (DSC). DSC studies were performed using a Mettler-Toledo DSC-1 equipped with a mechanical cooling system. Samples were placed in a 40 μL aluminum pan and sealed with a punctured lid. Melting and melt recrystallization behavior of various PEPI-POSS were studied by heating the sample from 25°C to a temperature about 30°C above the melting temperature with a rate of 20°C/min, and held for one minute, then cool back to 25°C at 20°C/min. All experiments were conducted in a nitrogen atmosphere. For phenylethynyl reaction studies, samples were heated from 100-500°C with heating rates of 2, 5, 10 and 20°C/min under a nitrogen atmosphere. Fourier Transform-Infrared spectroscopy (FT-IR) data was obtained using a Varian-Digilab FTS3000 equipped with a liquid nitrogen cooled mercury cadmium telluride detector. Samples were prepared by mixing ~2 mg of sample with ~80 mg of KBr, and pressed into 7 mm diameter discs.

## RESULTS AND DISCUSSION

### Synthesis

The methods devised to synthesize the three difunctional PEPI-POSS materials illustrated in Figure 1 are shown in Scheme 1 (Ph<sub>8</sub>bisPEPI-POSS) and Scheme 2 (Ph<sub>7</sub>diPEPI-POSS and

Ibu<sub>7</sub>diPEPI-POSS). To make Ph<sub>8</sub>bisPEPI-POSS, which has an architecture that can put a POSS cage directly into the backbone of a cross-linked network, a dichlorosilane with a protected aniline group was required for reaction with the relatively new phenylPOSS tetra silanol. ((N-trimethylsilyl)<sub>2</sub>-aniline-4-(dichloromethylsilane) was synthesized in high yield from (N-trimethylsilyl)<sub>2</sub>-4-bromoaniline by generating a Grignard reagent that was subsequently metathesized with methyltrichlorosilane. Figure 2a shows the <sup>29</sup>Si NMR spectrum of this compound: as expected there are just two peaks at +18.9 and +5.2 ppm in a ratio of 1:2 for the dichloromethylaniline and the trimethylsilyl silicons. Figure 3a displays the <sup>13</sup>C NMR spectrum. There are the expected 4 aromatic and two silyl methyl peaks.

This dichlorosilane is cleanly reacted with Ph<sub>8</sub>tetrasilanolPOSS in the presence of a small excess of triethylamine to promote the formation of a POSS with two protected amines. This molecule is deprotected with acid to generate equal amounts of cis- and trans-Ph<sub>8</sub>bisaniline-POSS; their structures and <sup>29</sup>Si NMR spectra are shown in figure 2b-d. Due to differences in solubility, it is possible to get reasonable separation of these isomers by crystallization. The C<sub>2h</sub> symmetry trans-isomer (figure 2c) shows an expected three <sup>29</sup>Si resonances at -29.9, -78.4 and -79.5 ppm in a ratio of 2:4:4. The C<sub>2v</sub> symmetry cis-isomer (figure 2d) shows an expected four <sup>29</sup>Si resonances at -29.9, -78.4, -79.3 and -79.7 ppm in a ratio of 2:4:2:2. Theoretically, one would expect to see seven resonances in spectrum 2b, but because of the very similar chemical environments for these two isomers, some of the cis- and trans-isomer resonances are isochronous (overlapping). This overlapping of similar chemical environment signals has been reported for other derivatives made from the POSS tetrol<sup>35</sup>. Based on symmetry arguments, the peak assignments are as follows: at -29.9 ppm (2 Si) are the aniline D-silicon atoms<sup>32</sup>; at -78.4 (4 Si) are the cage silicon atoms closest to the aniline silicon; at -79.5 (4 Si) are the trans-isomer's

central silicon atoms; and at  $-79.3$  (2 Si) and  $-79.7$  (2 Si) are the cis-isomer's central silicon atoms. The  $^{13}\text{C}$  NMR spectrum of the isomeric mixture is displayed in figure 3b. While it is not possible to assign all the overlapping aromatic resonances, the single methyl carbon peak at 0.3 ppm is a clear indication of purity and that the amines are fully deprotected (SiMe<sub>3</sub> groups are absent).

The isomeric cis/trans mixture of Ph<sub>8</sub>bisaniline-POSS was reacted with PEPA to generate the desired Ph<sub>8</sub>bisPEPI-POSS. The  $^{29}\text{Si}$  NMR spectrum is displayed in figure 2e. A small upfield shift of the D-silicon is observed (Figure 2e), but the other silicon resonances remain approximately the same. The  $^{13}\text{C}$  NMR (Figure 3c) shows several peaks indicative of the addition of PEPA, including two overlapping carbonyl resonances at 166.4 and 166.3 ppm, as well as two alkyne resonances at 87.7 and 94.2 ppm. In addition, the aromatic carbon alpha to the nitrogen also shows a significant upfield shift, as the primary amine converts to a tertiary imide. Along with the NMR data, FT-IR studies confirm the structure. The IR spectrum of Ph<sub>8</sub>bisPEPI-POSS shows imide carbonyl absorption peaks at 1727 and 1779 cm<sup>-1</sup>. Other important peaks include an absorbance at 2213 cm<sup>-1</sup>, which corresponds to an alkyne bond stretch and an absorbance at 1367 cm<sup>-1</sup>, which is attributed to an aromatic-imide carbon-nitrogen stretch.

The synthesis of the Ph<sub>7</sub>diPEPI-POSS and Ibu<sub>7</sub>diPEPI-POSS compounds is shown in Scheme 2, and  $^{29}\text{Si}$  NMR spectra related to the synthesis of the phenyl derivative are displayed in figure 4. To make R<sub>7</sub>diPEPI-POSS, which have an architecture that can put a POSS cage pendent to the backbone of a cross-linked network, a monochlorosilane with two protected aniline groups was required for reaction with a POSS-monosilanol. Di((N-trimethylsilyl)<sub>2</sub>-aniline)-4,4'-(chloromethylsilane) was synthesized in high yield from (N-trimethylsilyl)<sub>2</sub>-4-

bromoaniline by generating a Grignard reagent that was subsequently metathesized with half an equivalent of methyltrichlorosilane. Figure 4a shows the  $^{29}\text{Si}$  NMR spectrum of this compound: as expected there are just two peaks at +10.7 and +4.8 ppm in a ratio of 1:4 for the chloromethyldianiline and the trimethylsilyl silicons.

The POSS monosilanol,  $\text{R}_7\text{Si}_8\text{O}_{12}(\text{OH})$  is made by reacting POSS trisilanol,  $\text{R}_7\text{Si}_7\text{O}_9(\text{OH})_3$ , with tetrachlorosilane and then hydrolyzing the remaining silicon-chloride bond. The  $^{29}\text{Si}$  NMR spectrum of the phenyl derivative is displayed in figure 4b. There are three resonances near -78 ppm in the expected 3:3:1 ratio for the seven T-type cage silicon atoms, in three inequivalent chemical environments. There is one silicon peak near -100 ppm for the Q-type silicon containing the silanol functionality.

The di((n-trimethylsilyl)<sub>2</sub>-aniline)-4,4'-chloromethylsilane was grafted to the POSS monosilanol using a slight excess of  $\text{NEt}_3$  to both catalyze the reaction and drive it to completion by removal of HCl. The T- type silicon resonances shift slightly to give two resonances in a ratio of 3:4 while the Q- type silicon resonance shifts from -100 to -109 ppm (Figure 4c). There is also an M-type silicon resonance at -8.1 ppm which displays a typical 20 ppm upfield shift for replacement of a Si-Cl bond with a Si-O bond. Upon addition of PEPA, the  $^{29}\text{Si}$  NMR (Figure 4d) is similar to that of the diamines, with only a slight shift of the M-silicon to -8.7 ppm. Carbon NMR and FT-IR also confirms the addition of PEPA.

The monofunctional POSS compound,  $\text{Ph}_7\text{PEPI-POSS}$ , was synthesized as outlined in the experimental section. This chemistry is very similar what was just discussed. A Grignard reagent made from (N-trimethylsilyl)<sub>2</sub>-4-bromoaniline, was added to  $\text{SiCl}_4$  to make (N-trimethylsilyl)<sub>2</sub>-aniline-4-trichlorosilane. Its  $^{29}\text{Si}$  NMR spectrum displays 2 peaks in a ratio of 2:1 at +5.5 ppm ( $\text{SiMe}_3$ ) and at -0.8 ppm ( $\text{SiCl}_3$ ). This molecule is reacted with phenylPOSS

trisilanol,  $\text{Ph}_7\text{Si}_7\text{O}_9(\text{OH})_3$ , and the TMS groups are removed with acid, to generate  $\text{Ph}_7\text{anilinePOSS}$ . The  $^{29}\text{Si}$  NMR spectrum has three resonances in a ratio of 1:4:3 at -77.0 ppm (aniline silicon), 78.3 and -78.5 ppm, (phenyl silicons). Once the PEPA group is attached, the silicon attached to the aniline group shifts from -77.0 to -78.7 ppm. Carbon NMR and FT-IR analysis also confirms the structure, with carbonyl and alkyne resonances and absorptions the similar as those outlined for  $\text{Ph}_8\text{bisPEPI-POSS}$ .

### **Thermal Characteristics**

As demonstrated using NMR, PEPI-POSS are well-defined chemicals. Hence, they are effectively imide oligomers with a monodisperse molecular weight. Therefore, DSC was used to examine thermal transitions such as melting and melt recrystallization of PEPI-POSS molecules prior to the onset temperature of phenylethynyl reactions. In the following, we present results of thermal characteristics of PEPI-POSS molecules as affected by the peripheral moiety, spacer group between PEPI and core of SiO cage, and architecture of PEPI attachment to the SiO core.

***POSS molecules with an isobutyl periphery.*** All POSS molecules containing the isobutyl periphery exhibited a first-order melt and recrystallization characteristics. Upon examining samples in the DSC crucible after the heating and cooling cycles, all isobutyl PEPI-POSS molecules show good melt flow characteristics in the aluminum DSC crucible. For comparison, the DSC of octaisobutyl-POSS ( $\text{Ibu}_8\text{-POSS}$ ) was obtained and found to exhibit a first-order solid-to-liquid melting transition. Upon heating, the onset of melting occurs at 263°C. Upon cooling at a rate of 20°C/min., the onset of melt recrystallization occurs at about 224°C.

The monofunctional PEPI-POSS molecules,  $\text{Ibu}_7\text{propylPEPI-POSS}$  (157°C) and  $\text{Ibu}_7\text{phenylPEPI-POSS}$  (238°C), have melting points lower than  $\text{Ibu}_8\text{-POSS}$ . This could be due to a reduction in POSS-POSS interactions when replacing one of the eight isobutyl groups with

either a propyl- or phenyl-PEPI group. Furthermore, the rigid phenyl group and the possible additional phenyl-phenyl interactions led to a higher melting temperature for Ibu<sub>7</sub>phenylPEPI-POSS as compared to Ibu<sub>7</sub>propylPEPI-POSS. This hypothesis was further verified by comparing the cooling curves. At a 20°C/min. cooling rate, an undercooling of about 70°C is required for Ibu<sub>7</sub>propylPEPI-POSS to form crystals, while only 60°C of undercooling was observed for Ibu<sub>7</sub>phenylPEPI-POSS. In addition, we compared the ratio of the exothermic crystallization peak,  $\Delta H_c$ , to the endothermic melting peak,  $\Delta H_m$ ; the value of this ratio is related to the degree of crystallization of a crystalline-forming molecule at the specified cooling condition. Results show that about 60% crystallization occurred for Ibu<sub>7</sub>propylPEPI-POSS and about 85% for Ibu<sub>7</sub>phenylPEPI-POSS. Studying a difunctional molecule, Ibu<sub>7</sub>diPEPI-POSS has a melting point at around 190°C. However, upon cooling at 20°C/min., only about 36% was crystallized and the extent of undercooling required to form crystals is similar to the Ibu<sub>7</sub>propylPEPI-POSS. The decrease in the degree of crystallization can be attributed the size of diPEPI functionality at the corner of POSS cage.

***POSS molecules with a phenyl periphery.*** The thermal transitions of POSS molecules with a phenyl periphery were different than those with the isobutyl periphery. The monofunctional Ph<sub>7</sub>phenylPEPI-POSS, when heated from room temperature to 500°C, shows only peaks associated with the exothermic reactions of phenylethyenyl. After cure, the sample remains in a powdery form, indicating a lack of flow in Ph<sub>7</sub>phenylPEPI-POSS upon heating at atmospheric pressure. This is similar to the octaphenyl-POSS (Ph<sub>8</sub>-POSS) where a very strong phenyl-phenyl interaction inhibits solid-to-liquid transition in a normal atmosphere.

The difunctional Ph<sub>7</sub>diPEPI-POSS is the only PhPOSS molecule reported in this study to exhibit a melting transition, which occurs at about 296°C. This is more than 100°C above

Ibu<sub>7</sub>diPEPI-POSS. This indicates that the phenyl periphery provides stronger POSS-POSS interactions than does the isobutyl. It is difficult to examine the kinetics of Ph<sub>7</sub>diPEPI-POSS to form crystals from the melt due to a partial overlap of reaction of phenylethyne at the melting temperature range. Altering the architecture of attachment of PEPI to the SiO core of POSS, Ph<sub>8</sub>bisPEPI-POSS shows a T<sub>g</sub> at 100°C. This “in-chain” morphology makes the crystallization of POSS more difficult as compared to those POSS molecules with difunctional PEPI at one corner. However, both difunctional PhPEPI-POSS molecules exhibit good flow characteristics upon heating above their thermal transitions at the atmospheric pressure.

***POSS molecules with eight phenylethyne groups.*** To better evaluate the influence of spacer group between the reactive PEPI and SiO core of POSS, octafunctional PEPI-POSS molecules were used. OctapropylPEPI-POSS has a melting temperature of 234°C, whereas octaphenylPEPI-POSS exhibits a glass transition temperature of 205°C. Both molecules show good flow upon heating past their respective thermal transitions. This observation is important for using these molecules as matrix materials in composite applications.

OctapropylPEPI-POSS can easily crystallize upon cooling from the melt. At a rate of 20°C/min., only 45°C of undercooling is needed to initiate crystallization, with 85 wt% transformed to the crystalline phase with continuous cooling. The lower undercooling and higher extent of crystallization of octapropylPEPI-POSS as compared to Ibu<sub>7</sub>propylPEPI-POSS, Ibu<sub>7</sub>phenylPEPI-POSS, and Ibu<sub>7</sub>diPEPI-POSS can be attributed to the identical chemical moiety surrounding to the SiO core of POSS.

### **Kinetics of PEPI-POSS Reactions**

A dynamic heating method was used to investigate reaction kinetics of phenylethyne for all PEPI-functionalized POSS molecules. Four different heating rates, ranging from 2 to 20°C

per minute were used. Analysis based on the  $n^{\text{th}}$  order kinetics model combined with the Arrhenius assumption for the temperature function of the reaction rate constant was performed on these dynamic heating curves.<sup>36</sup> Results of this analysis are tabulated and shown in Tables 2 and 3. Typical exothermic profiles representing reactions of phenylethynyl for the different PEPI-POSS molecules are also shown in Figures 5 to 10. In the  $n^{\text{th}}$  order kinetics model, the reaction rate constant and value of  $n$  are determined as a function of temperature. Since the value of  $n$  varies with temperature, the activation energy is affected by the temperature. However, the activation energy for a specific PEPI-POSS molecule, as listed in Table 3, is associated with the maximum cure rate temperature, the peak temperature of the exothermic reaction peak. The validity of the activation energy obtained was verified, as the extent of reaction at the peak maximum with respect to the overall reaction was found to be independent of the heating rate. Additional discussions regarding the effect of peripheral moiety, spacer group between PEPI and the SiO core, and architecture of POSS on the reaction kinetics of phenylethynyl follow.

***POSS peripheral effects.*** In Figure 5, the reaction profile of Ibu<sub>7</sub>phenylPEPI-POSS was compared to Ph<sub>7</sub>phenylPEPI-POSS. As shown, the curing profile of Ph<sub>7</sub>phenylPEPI-POSS is relatively broad and has at least two discernable peaks. Since the number of reactive phenylethynyl groups per POSS molecule is known, the normalized exothermic heat flow per mole of POSS was plotted versus temperature. The total heat of reaction,  $\Delta H_{\text{Rxn}}$ , under different heating rates varies a little more for Ph<sub>7</sub>phenylPEPI-POSS, as compared to Ibu<sub>7</sub>phenylPEPI-POSS,  $107 \pm 35$  versus  $175 \pm 11$  kJ/mole. Furthermore, the activation energy for the maximum curing rate is higher for Ph<sub>7</sub>phenylPEPI-POSS as compared to Ibu<sub>7</sub>phenylPEPI-POSS, 203 versus 105 kJ/mole, as is the peak reaction temperature at the same heating rate. The higher activation energy could be partially attributed to the thermal characteristics of Ph<sub>7</sub>phenylPEPI-

POSS prior to the phenylethynyl reaction, as it lacks any kind of flow characteristics as previously mentioned. In addition, this lack of flow may also contribute to the larger variance observed in the value of  $\Delta H_{Rxn}$  at different heating rates. However, one of most critical observations is that the mean value of  $\Delta H_{Rxn}$  is smaller for POSS with the phenyl periphery than that with the isobutyl. To further examine this observation, reaction kinetics of difunctional PEPI-POSS with phenyl and isobutyl peripheries were evaluated.

The reaction profiles for difunctional PEPI-POSS molecules with phenyl and isobutyl peripheries are shown in Figure 6. Unlike monoPEPI-POSS, both Ph<sub>7</sub>diPEPI-POSS and Ibu<sub>7</sub>diPEPI-POSS exhibit good flow characteristics prior to any phenylethynyl reactions. Hence, no significant variance of the values of  $\Delta H_{Rxn}$  at different heat rates was observed for both Ph<sub>7</sub>diPEPI-POSS and Ibu<sub>7</sub>diPEPI-POSS. The activation energies at maximum curing rate for both POSS molecules were also similar to each other, 149 and 146 kJ/mole, respectively. However, similar to monoPEPI-POSS molecules, the reaction peak temperature of Ph<sub>7</sub>diPEPI-POSS is higher than Ibu<sub>7</sub>diPEPI-POSS at the same heating rate. Values of  $\Delta H_{Rxn}$  are also smaller for Ph<sub>7</sub>diPEPI-POSS as compared to Ibu<sub>7</sub>diPEPI-POSS, 84 kJ/mole versus 163 kJ/mole. The reaction rate constant of phenylethynyl at a specific temperature is smaller for POSS with a phenyl periphery than POSS molecules with an isobutyl periphery, regardless of the functionality of the PEPI attached to the POSS core. Overall, it appears the phenyl periphery restricts or retards phenylethynyl reactions.

***PEPI-POSS spacer effects.*** Figure 7 shows the phenylethynyl reaction profiles of Ibu<sub>7</sub>propylPEPI-POSS and Ibu<sub>7</sub>phenylPEPI-POSS. Ibu<sub>7</sub>phenylPEPI-POSS has a higher extent of reaction before the peak maximum, 60%, as compared to Ibu<sub>7</sub>phenylPEPI-POSS, 51%, with both having similar values of peak reaction temperature at the same heating rates, as shown in Table

3. Infrared spectroscopy was used to determine the extent of loss of the alkyne group at the cure peak maximum for each of these molecules, using the  $1779\text{ cm}^{-1}$  carbonyl stretch as an internal reference. The  $\text{Ibu}_7\text{phenylPEPI-POSS}$  molecule had an 80% loss of the alkyne peak, whereas the  $\text{Ibu}_7\text{propylPEPI-POSS}$  molecule had a 72% loss of the alkyne peak at the cure peak maximum. The rate constant for  $\text{Ibu}_7\text{phenylPEPI-POSS}$  is higher than  $\text{Ibu}_7\text{propylPEPI-POSS}$  at temperatures below the cure peak maximum. These results suggest that it is easier for  $\text{Ibu}_7\text{phenylPEPI-POSS}$  to initiate the initial phenylethynyl polyene reaction as compared to  $\text{Ibu}_7\text{propylPEPI-POSS}$ , where the phenylethynyl group is attached to a more flexible spacer. However, these two POSS molecules are monofunctional, hence the subsequent reactions are limited. Therefore, the value for the overall  $\Delta H_{\text{Rxn}}$  is the same for both molecules. To further explore the influence of spacer group on the phenylethynyl reactions, octafunctional POSS molecules were investigated.

The reaction profiles of octaphenylPEPI-POSS and octapropylPEPI-POSS are shown in Figure 8. Unlike their monofunctional counterparts, both octafunctional POSS molecules exhibit a more asymmetrical reaction profile with a much longer tail at the higher temperature region of reaction curves. This suggests that there exist multiple, complex reaction mechanisms after the initial polyene reaction, as the order of reaction changed from about 1.5 at  $340^\circ\text{C}$  to about 0.5 at  $390^\circ\text{C}$ . However, it appears that the octaphenylPEPI-POSS has two strongly overlapping broad peaks. The extent of the overlap becomes lesser as the heating rate increases, as shown in Figure 9. In Table 3, values of the low temperature peak, LTP, of octaphenylPEPI-POSS at different heating rates were similar to the value of reaction peak maximum of octapropylPEPI-POSS. Hence, the activation energies for both POSS molecules were also similar to each other. However, the extent of reaction was different from each other, 22 % versus 41%. Furthermore,

the rate constant for octaphenylPEPI-POSS was much lower than that of octapropylPEPI-POSS and the overall reaction was smaller for octaphenylPEPI-POSS as compared to octapropylPEPI-POSS, 95 versus 143 kJ/mole. These observations suggest that the flexibility of the spacer group between PEPI and the POSS core effects the extent of initial phenylethynyl reactions and the extent of cure increases as the spacer group become more flexible. Moreover as the number of phenylethynyl groups per POSS molecule increases, the reaction kinetics become diffusion controlled quicker than with difunctional POSS.

**Architectural effects.** The architecture of the PEPI attachment to the POSS core was investigated by comparing Ph<sub>8</sub>bisPEPI-POSS and Ph<sub>7</sub>diPEPI-POSS, as shown in Figure 10. It is apparent that the onset of reaction temperature is lower for Ph<sub>8</sub>bisPEPI-POSS as compared to Ph<sub>7</sub>diPEPI-POSS and the overall  $\Delta H_{Rxn}$  is higher for Ph<sub>8</sub>bisPEPI-POSS, 134 kJ/mole versus 84 kJ/mole. The reaction rate constants are also much higher for Ph<sub>8</sub>bisPEPI-POSS during the entire temperature range of phenylethynyl reactions. This suggests that the “in-chain” morphology of Ph<sub>8</sub>bisPEPI-POSS allows for a more completed phenylethynyl cure as compared to that of the “T-shaped” Ph<sub>7</sub>diPEPI-POSS.

**Comparison to HFPE oligoimides.** Reaction kinetics of PEPI-POSS were compared to those hexafluorophenylethynyl oligoimides, HFPE-n-9 and HFPE-n-1. Based on the results tabulated in Table 2 and 3, it is clear that the phenylethynyl reaction kinetics were comparable. Therefore, PEPI-POSS can be co-cured with HFPE oligoimides without any modifications on the curing temperature profile used for composite processing.

## CONCLUSIONS

A series of phenylethynyl-functionalized POSS molecules were synthesized and studied to determine the effect of the POSS periphery, PEPI-POSS spacer group, and POSS architecture on the phenylethynyl curing reaction. It was shown that these POSS modifications had an impact on activation energy, heat of fusion, and the overall reaction profile. Changing the POSS periphery from isobutyl to phenyl resulted in a restriction or retardation of phenylethynyl reactions. Changing the PEPI-POSS spacer from a flexible propyl to a less flexible phenyl had an effect on the extent of initial curing with mono and octafunctionalPOSS molecules and caused a decrease in the extent of cure with octafunctionalPOSS molecules. Architecturally, changing POSS from an “in-chain” structure to a “pendant” structure resulted in a decrease in the extent of curing reaction. The kinetics of POSS molecules compare favorably with oligoimides, which will allow for co-curing reactions in composites. Overall, the POSS periphery, architecture, and spacer groups have an important impact on their curing reactions.

## **ACKNOWLEDGEMENTS**

This work was supported by the Air Force Office of Scientific Research, Polymer Matrix Composites program, FA9550-08-1-0213, under Dr. Charles Lee.

## REFERENCES

1. Joshi, M. and Butola, B. *J. Macromol. Sci. Part C: Polym. Rev.* **2004**, *44*, 389-410.
2. Li, G., Wang, L. Ni, H., Pittman Jr., C. *J. Inorg. Organomet. Polym.* **2001**, *11*, 123-154.
3. Mammeri, F., Bourhis, E., Rozes, L., and Sanchez, C. *J. Mater. Chem.* **2005**, *15*, 3787-3811.
4. Sanchez, C., Julian, B., Belleville, P., and Popall, M. *J. Mater. Chem.* **2005**, *15*, 3559-3592.
5. Sanchez, C., Soler-Illia, G., Ribot, F., Lalot, T., Mayer, C., Cabuil, V. *Chem. Mater.* **2001**, *13*, 3061-3083.
6. Phillips, S., Haddad, T., and Tomczak, S. *Curr. Opin. Solid State Mater. Sci.* **2004**, *8*, 21-29.
7. Gilman, J., Schlitzer, D., Lichtenhan, J. *J. Appl. Polym. Sci.* **1996**, *60*, 591-596.
8. Leu, C., Reddy, G., Wei, K., Shu, C. *Chem. Mat.* **2003**, *15*, 2261-2265.
9. Wright, M., Petteys, B., Guenther, A., Fallis, S., Yandek, G., Tomczak, S., Minton, T., Brunsvolk, A. *Macromolecules* **2006**, *39*, 4710-4718.
10. Brunsvolk, A., Minton, T., Gouzman, I., Grossman, E., Gonzalez, R. *High Perform. Polym.* **2004**, *16*, 303-318.
11. Pielichowski, K., Njuguna, J., Janowski, B., and Pielichowski, J. *Adv. Polym. Sci.* **2006**, *201*, 225-296.
12. Wu, J., and Mather, P. *Polym. Rev.* **2009**, *49*, 25-63.
13. Laine, R. *J. Mater. Chem.* **2005**, *15*, 3725-3744.
14. Soh, M., Sellinger, A., and Yap, A. *Curr. Nanosci.* **2006**, *2*, 373-381.
15. Wu, S., Hayakawa, T., Kakimoto, M., and Oikawa, H. *Macromolecules* **2008**, *41*, 3481-3487.
16. Wright, M., Schorzman, D., Feher, F., Jin, R. *Chem. Mat.* **2003**, *15*, 264-268.
17. Seurer, B. and Coughlin, B. *Macromol. Chem. Phys.* **2008**, *209*, 1198-1209.
18. Seurer, B. and Coughlin, E.B. *Macromol. Chem. Phys.* **2008**, *209*, 2040-2048.
19. Haddad, T., Viers, B., and Phillips, S. *J. Inorg. Organomet. Polym.* **2001**, *127*, 155-164.

20. Drazkowski, D., Lee, A., Haddad, T., and Cookson, D. *Macromolecules* **2006**, *39*, 1854-1863.
21. Bolln, C., Tsuchida, A., Frey, H., and Mulhaupt, R. *Chem. Mat.* **1997**, *9*, 1475-1479.
22. Li, Y. and Morgan, R. *J. Appl. Polym. Sci.* **2006**, *101*, 4446-4453.
23. Fang, X., Xie, X., Simone, C., Stevens, M., and Scola, D. *Macromolecules* **2000**, *33*, 1671-1681.
24. Roberts, C., Apple, T., and Wwnek, G. *J. Polym. Sci. Part A: Polym. Chem.* **2000**, *38*, 3486-3497.
25. Fang, X., Rogers, D., Scola, D., and Stevens, M. *J. Polym. Sci. Part A: Polym. Chem.* **1998**, *36*, 461-470.
26. Cho, D. and Drzal, L. *J. Appl. Polym. Sci.* **2000**, *76*, 190-200.
27. Russell, J. and Kardos, J. *Polym. Composites* **1997**, *18*, 595-612.
28. Connell, J., Smith, J., Hergenrother, P., and Criss, J. *High Perform. Polym.* **2003**, *15*, 375-394.
29. Serafini, T., Delvigs, P. and Lightsey, G. *J. Appl. Polym. Sci.* **1972**, *16*, 905-915.
30. Lee, A. *High Perform. Polym.* **1996**, *8*, 475-489.
31. Chuang, K., Bowman, C., Tsotsis, T., and Arendt, C. *High Perform. Polym.* **2003**, *15*, 459-472.
32. Simone, C. and Scola, D. *High Perf. Polym.* **2003**, *15*, 473-501.
33. Kim, S., Lu, M., and Shim, M. *Polym. J.* **1998**, *30*, 90-94.
34. Brook, M. *Silicon in Organic, Organometallic, and Polymer Chemistry*. Wiley Interscience: New York, **2000**, 12-13.
35. Hoque, M., Kakihana, Y., Shinke, S., and Kawakami, Y. *Macromolecules* **2009**, *42*, 3309-3315.
36. Lu, M., Shim, M., and Kim, S. *J. Therm. Anal. Cal.* **1999**, *58*, 701-709.

## FIGURE CAPTIONS

- Figure 1. Structures of PEPI-functionalized compounds investigated.
- Figure 2.  $^{29}\text{Si}$  NMR of (a) (n-trimethylsilyl)<sub>2</sub>-aniline-4-dichloromethylsilane (b) Ph<sub>8</sub>bisaniline-POSS and (c) Ph<sub>8</sub>bisPEPI-POSS.
- Figure 3.  $^{13}\text{C}$  NMR of (a) Ph<sub>8</sub>bisaniline-POSS; and (b) Ph<sub>8</sub>bisPEPI-POSS.
- Figure 4.  $^{29}\text{Si}$  NMR of (a) bis((n-trimethylsilyl)<sub>2</sub>-aniline)-4,4'-chloromethylsilane (b) Ph<sub>7</sub>OH-POSS (c) Ph<sub>7</sub>diamine-POSS and (d) Ph<sub>7</sub>diPEPI-POSS.
- Figure 5. Phenylethynyl reaction profiles of Ph<sub>7</sub>phenylPEPI-POSS (solid line) and Ibu<sub>7</sub>phenylPEPI-POSS (dashed line) with a heating rate of 10°C per minute. The y-axis is the normalized heat flow with respect to the mole of POSS. Each POSS has one PEPI group.
- Figure 6. Phenylethynyl reaction profiles of Ph<sub>7</sub>diPEPI-POSS (solid line) and Ibu<sub>7</sub>diPEPI-POSS (dashed line), with a heating rate of 10°C per minute. The y-axis is the normalized heat flow with respect to the moles of POSS. Each POSS molecule has two PEPI groups.
- Figure 7. Phenylethynyl reaction profiles of Ibu<sub>7</sub>phenylPEPI-POSS (solid line) and Ibu<sub>7</sub>propylPEPI-POSS (dashed line), with a heating rate of 10°C per minute. The y-axis is the normalized heat flow with respect to the moles of POSS. Each POSS molecule has one PEPI group.
- Figure 8. Phenylethynyl reaction profiles of OctaphenylPEPI-POSS (solid line) and OctapropylPEPI-POSS (dashed line), with a heating rate of 10°C per minute. The y-axis is the normalized heat flow with respect to the moles of POSS. Each POSS molecule has eight PEPI groups.
- Figure 9. Phenylethynyl reaction profiles of octaphenylPEPI-POSS, at 20°C/min (solid line), 10°C/min (dashed line), 5°C/min (dotted line), and 2°C/min (dashed-dotted line) heating rates.
- Figure 10. Phenylethynyl reaction profiles of Ph<sub>7</sub>diPEPI-POSS (solid line) and Ph<sub>8</sub>bisPEPI-POSS (dashed line), with a heating rate of 10°C per minute. The y-axis is the normalized heat flow with respect to the moles of POSS. Each POSS molecule has two PEPI groups.

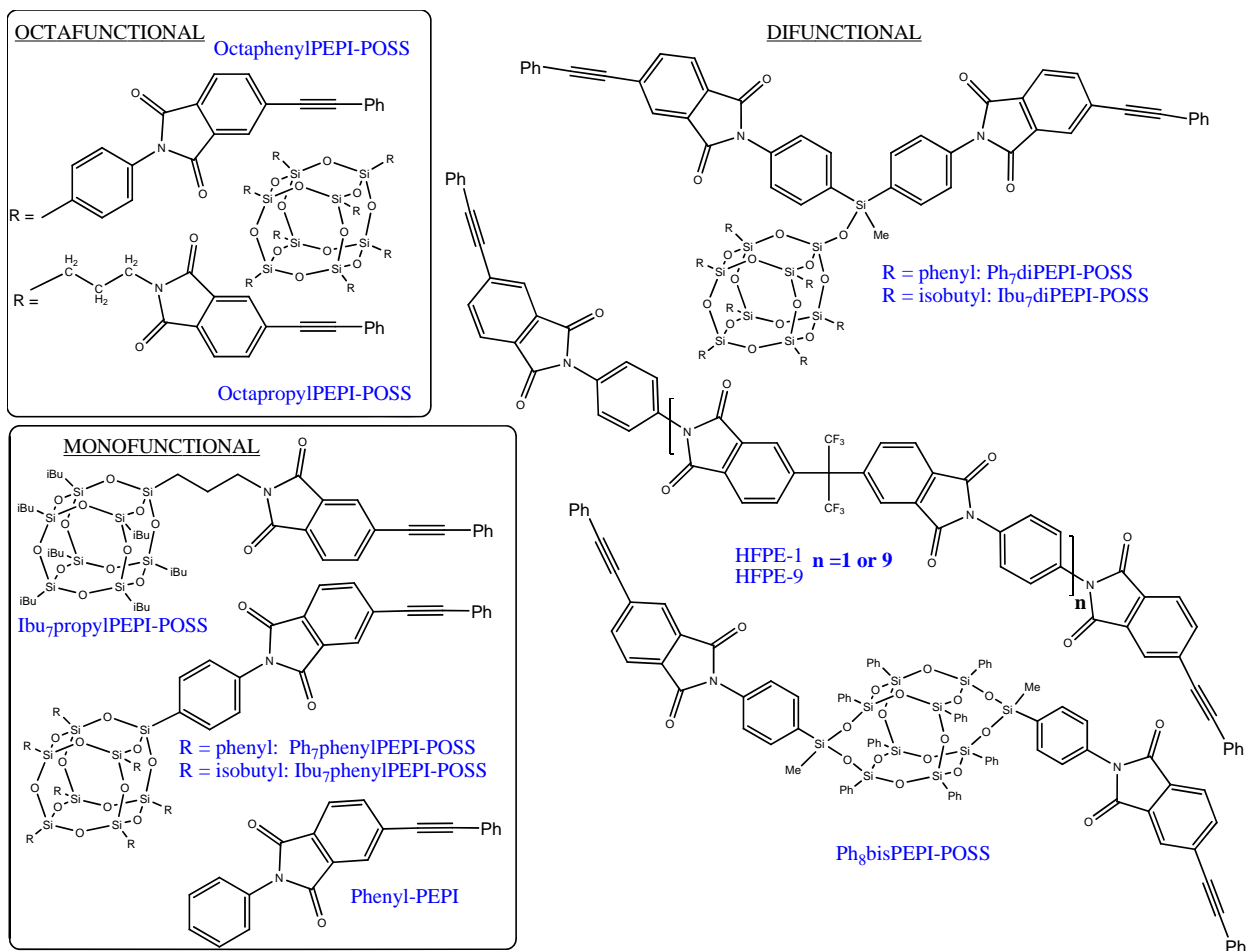


Figure 1. Structures of PEPI-functionalized compounds investigated.

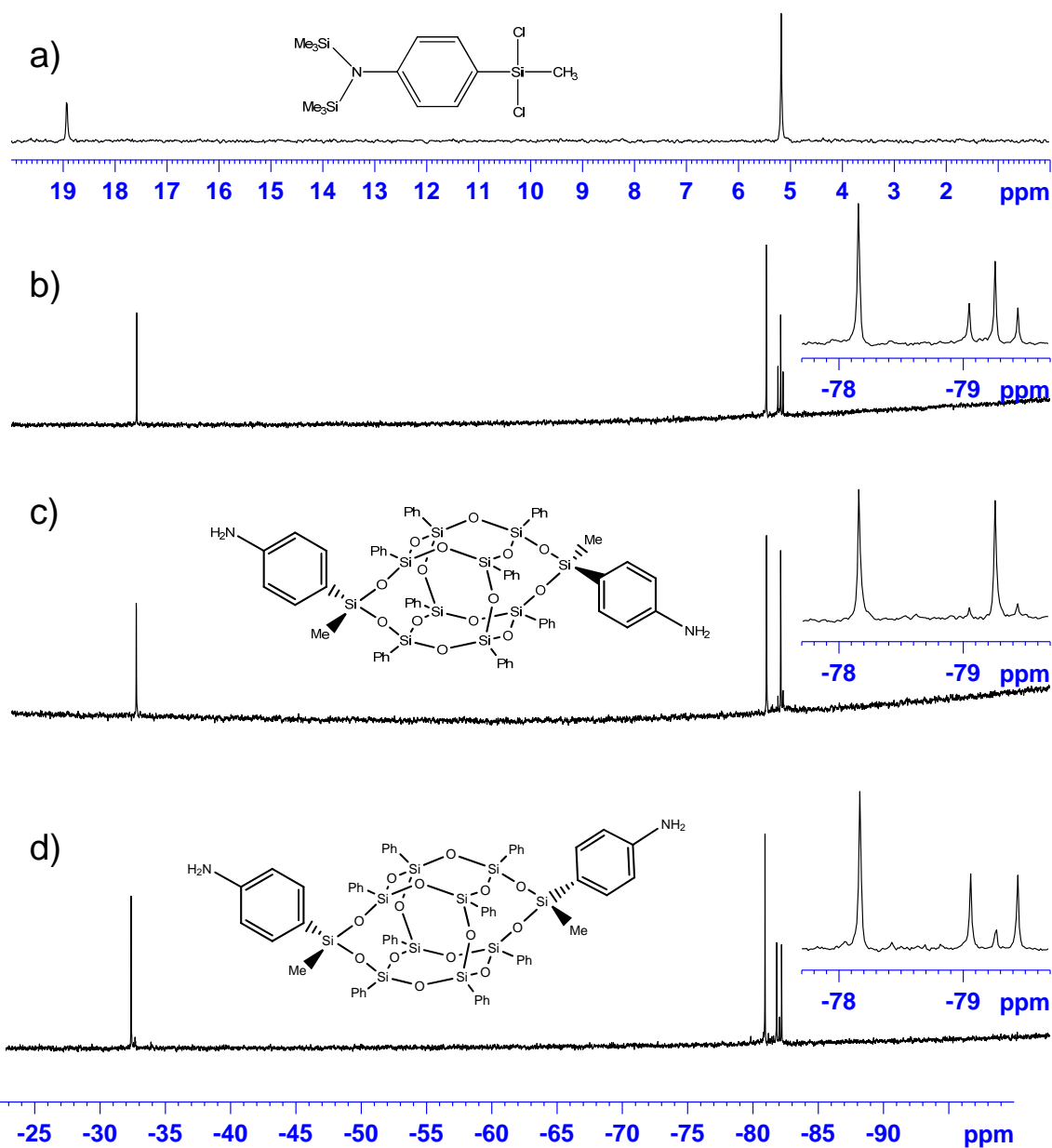


Figure 2.  $^{29}\text{Si}$  NMR of (a)  $(n\text{-trimethylsilyl})_2\text{-aniline-4-dichloromethylsilane}$ ; (b) *cis/trans* mixture of  $\text{Ph}_8\text{bisaniline-POSS}$ ; (c) mostly *trans*- $\text{Ph}_8\text{bisaniline-POSS}$ , (d) mostly *cis*- $\text{Ph}_8\text{bisaniline-POSS}$ . The insets show the effect of the symmetry of the isomeric structures on the four central silicon atoms.

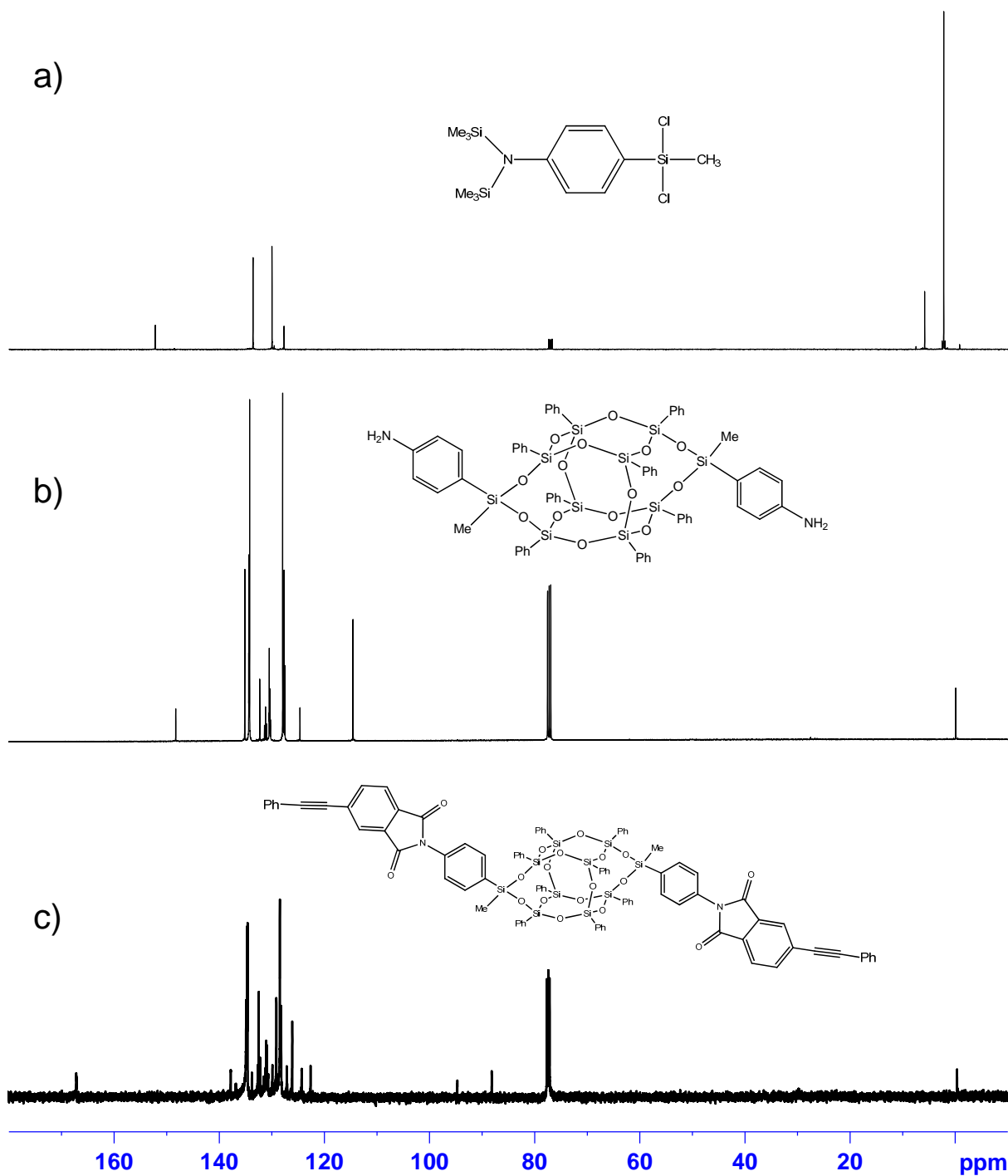


Figure 3.  $^{13}\text{C}$  NMR of (a) (n-trimethylsilyl) $_2$ -aniline-4-dichloromethylsilane; (b)  $\text{Ph}_8$ bis(aniline)-POSS (cis and trans isomers); and (c)  $\text{Ph}_8$ bis(PEPI)-POSS (cis and trans isomers).

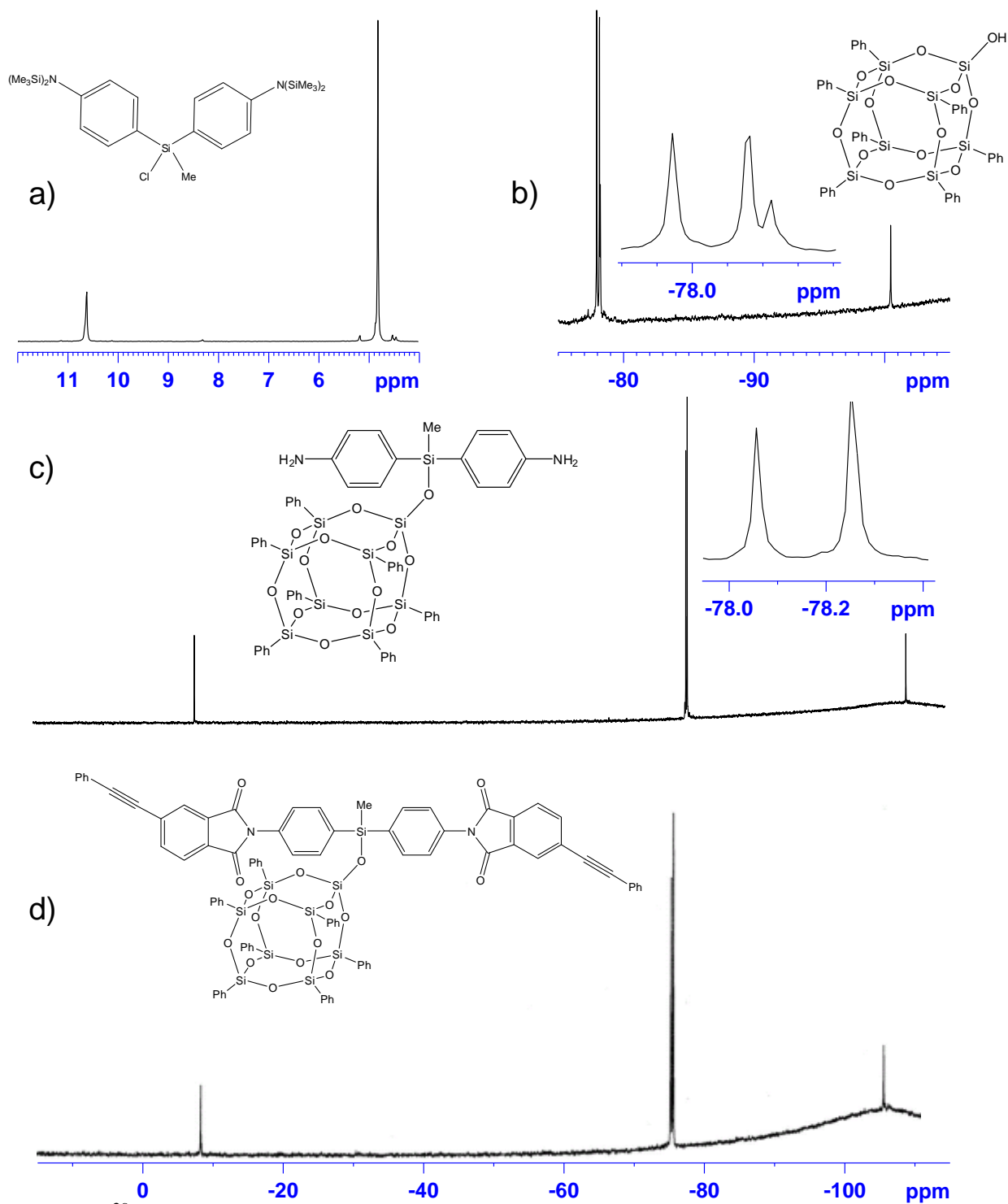


Figure 4.  $^{29}\text{Si}$  NMR of (a) bis((n-trimethylsilyl) $_2$ -aniline)-4,4'-chloromethylsilane (b) Ph $_7$ OH-POSS (c) Ph $_7$ diamine-POSS and (d) Ph $_7$ diPEPI-POSS.

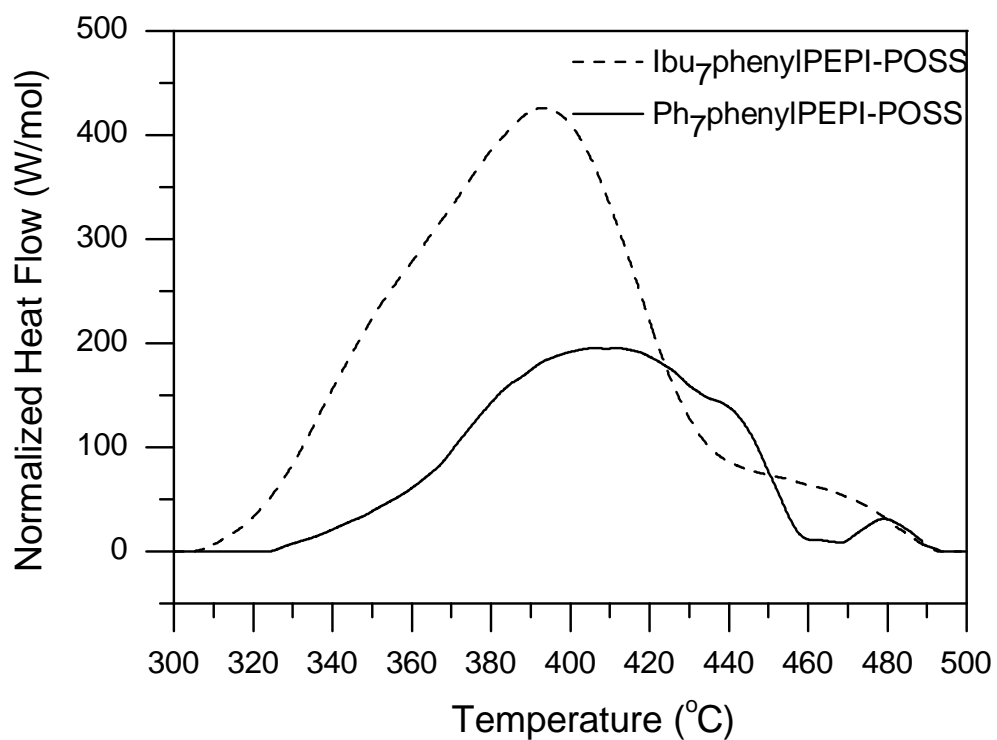


Figure 5. Phenylethynyl reaction profiles of Ph<sub>7</sub>phenylPEPI-POSS (solid line) and Ibu<sub>7</sub>phenylPEPI-POSS (dashed line) with a heating rate of 10°C per minute. The y-axis is the normalized heat flow with respect to the mole of POSS. Each POSS has one PEPI group.

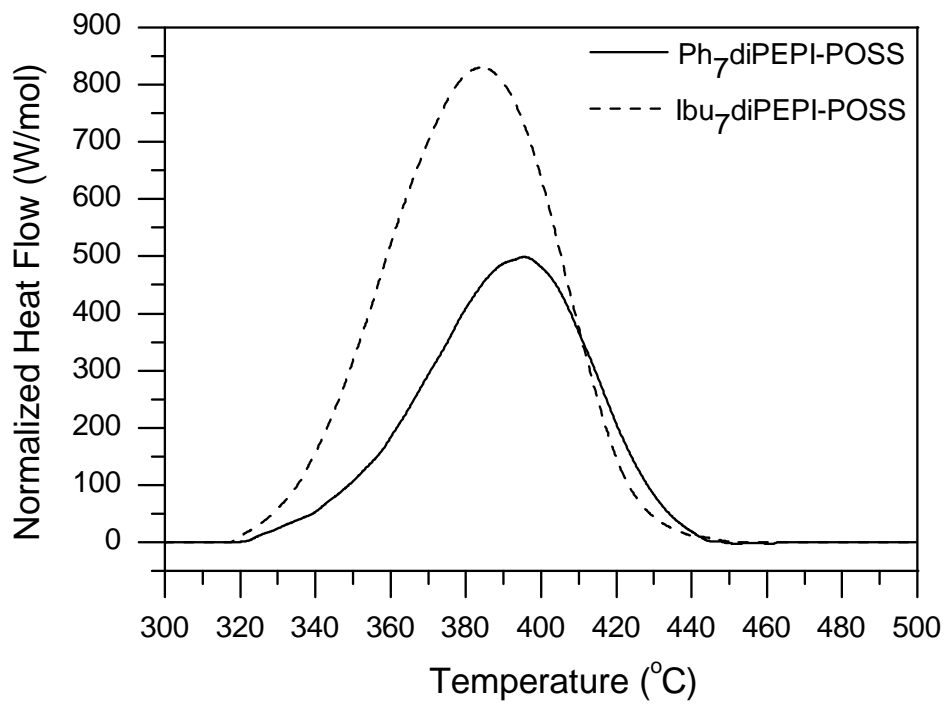


Figure 6. Phenylethynyl reaction profiles of Ph<sub>7</sub>diPEPI-POSS (solid line) and Ibu<sub>7</sub>diPEPI-POSS (dashed line), with a heating rate of 10°C per minute. The y-axis is the normalized heat flow with respect to the moles of POSS. Each POSS molecule has two PEPI groups.

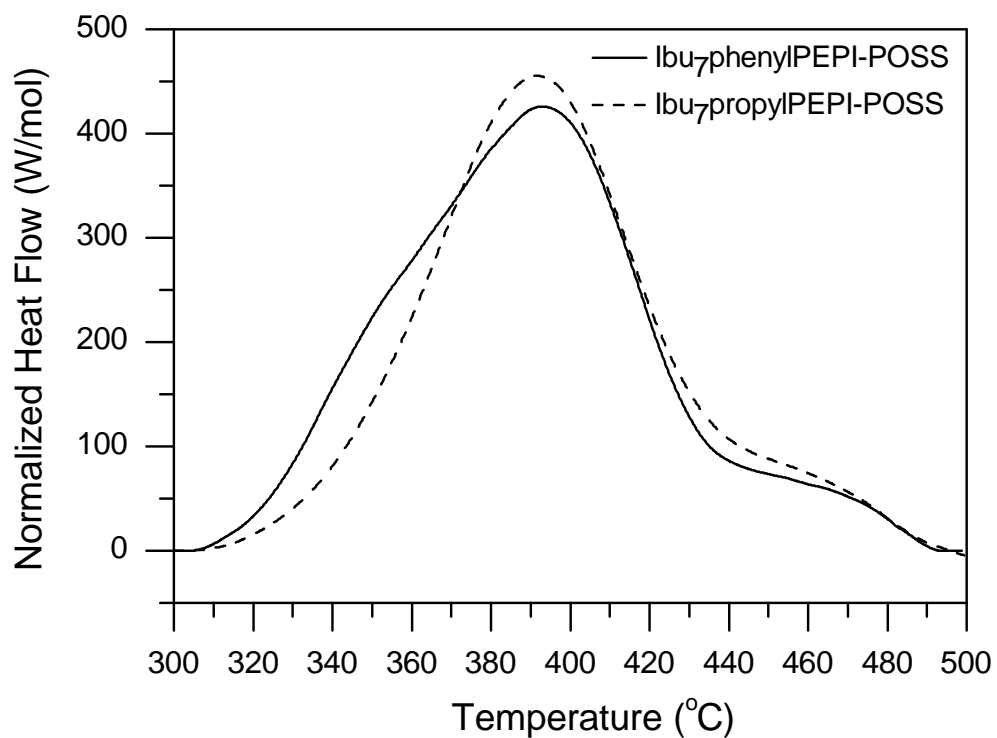


Figure 7. Phenylethynyl reaction profiles of Ibu<sub>7</sub>phenylPEPI-POSS (solid line) and Ibu<sub>7</sub>propylPEPI-POSS (dashed line), with a heating rate of 10°C per minute. The y-axis is the normalized heat flow with respect to the moles of POSS. Each POSS molecule has one PEPI group.

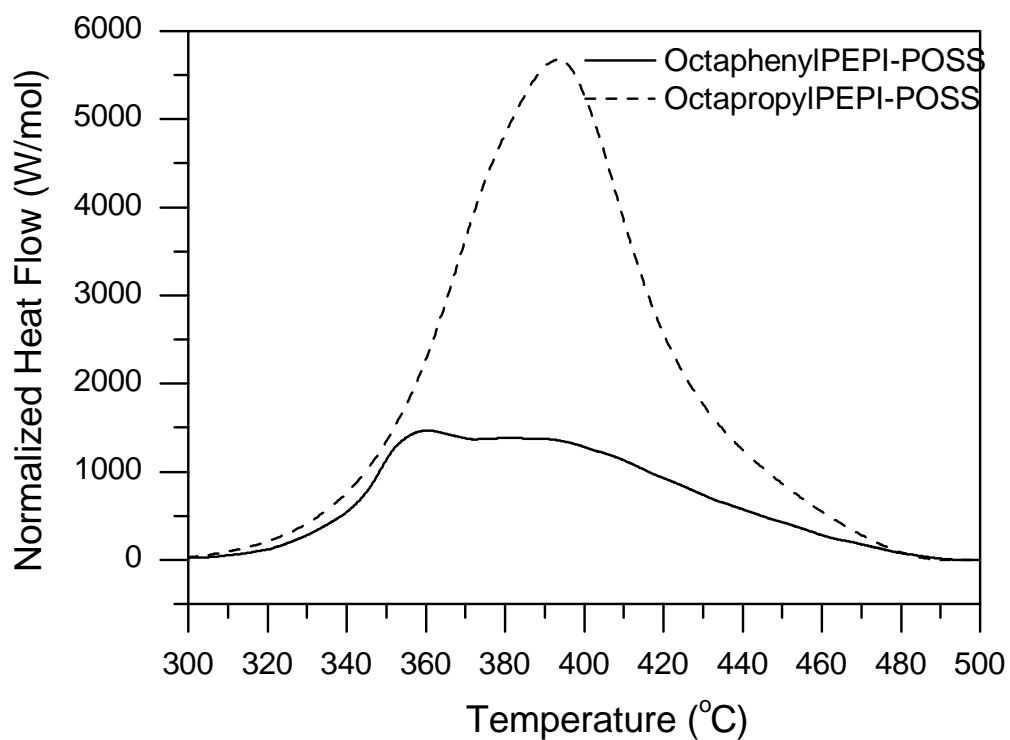


Figure 8. Phenylethynyl reaction profiles of OctaphenylPEPI-POSS (solid line) and OctapropylPEPI-POSS (dashed line), with a heating rate of 10°C per minute. The y-axis is the normalized heat flow with respect to the moles of POSS. Each POSS molecule has eight PEPI groups.

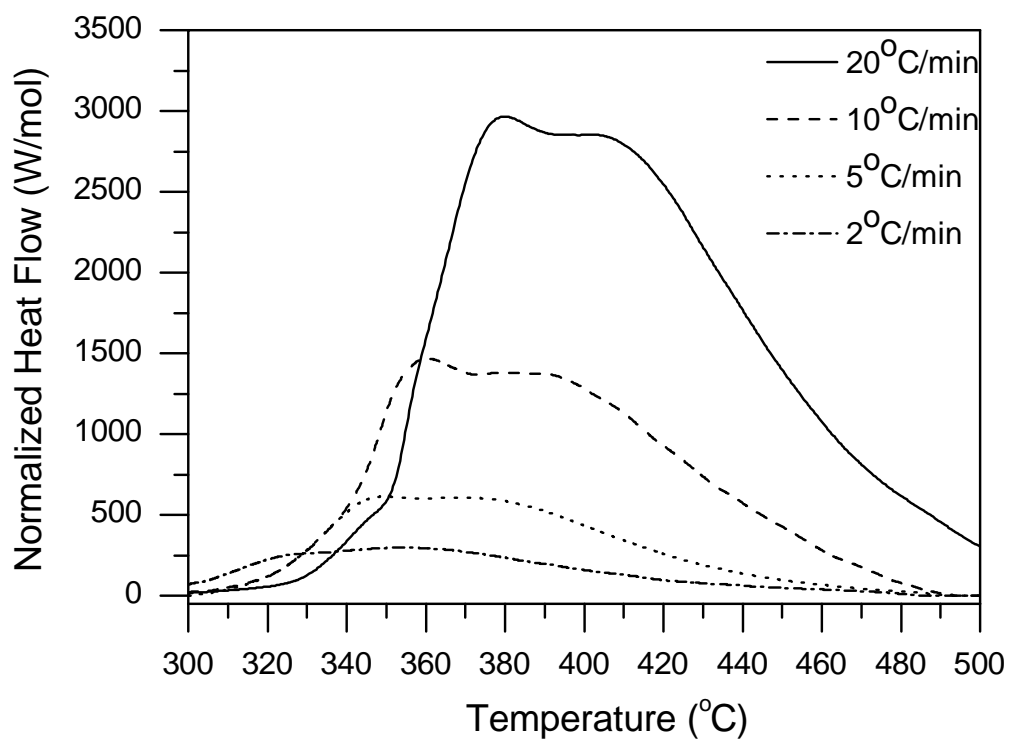


Figure 9. Phenylethynyl reaction profiles of octaphenylPEPI-POSS, at 20°C/min (solid line), 10°C/min (dashed line), 5°C/min (dotted line), and 2°C/min (dashed-dotted line) heating rates.

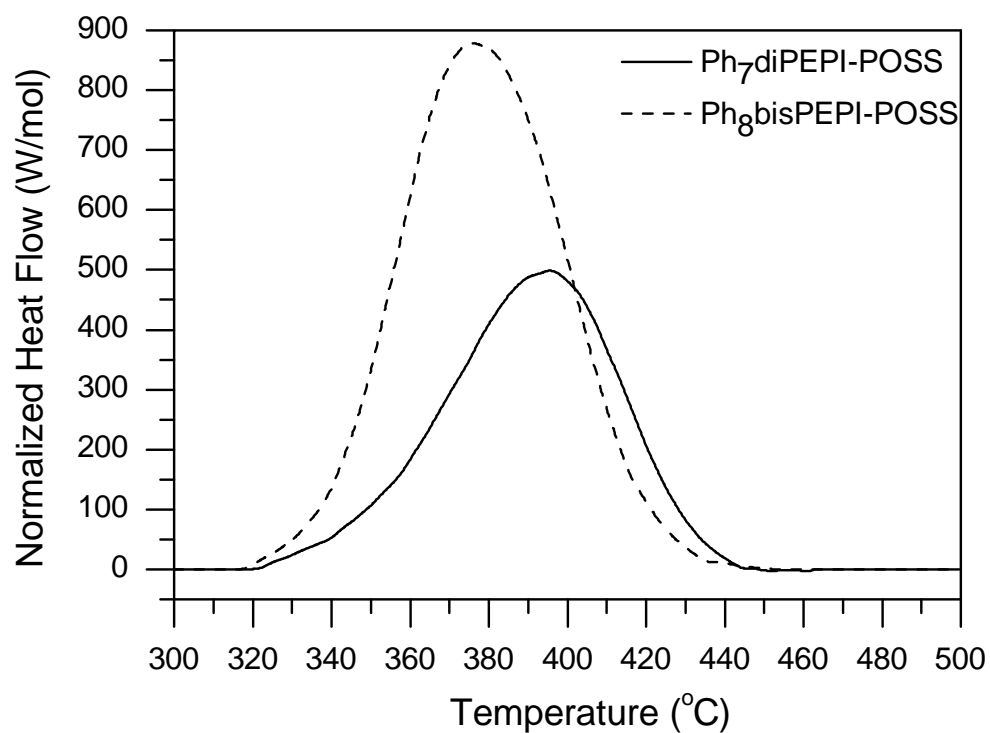
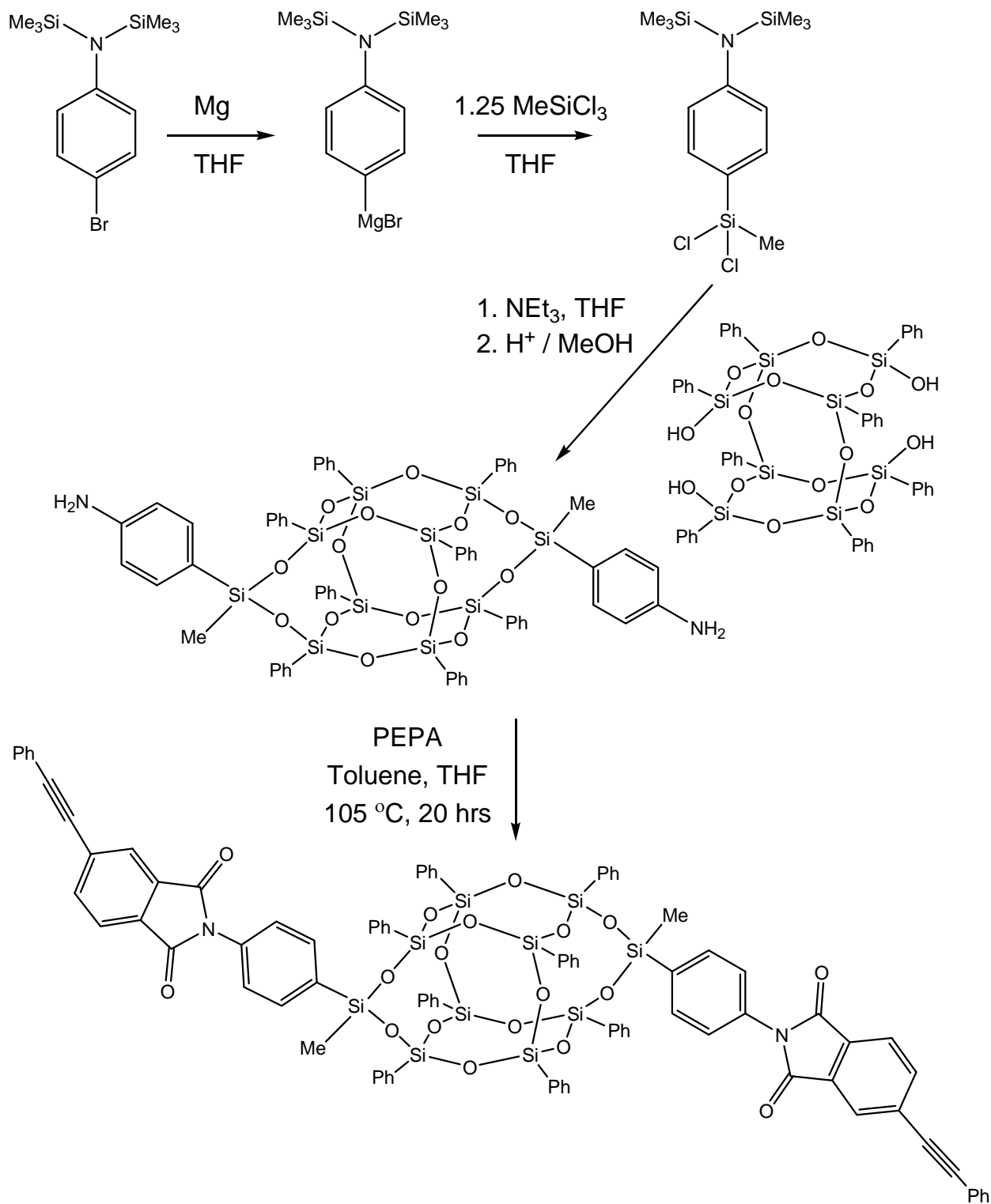


Figure 10. Phenylethynyl reaction profiles of Ph<sub>7</sub>diPEPI-POSS (solid line) and Ph<sub>8</sub>bisPEPI-POSS (dashed line), with a heating rate of 10°C per minute. The y-axis is the normalized heat flow with respect to the moles of POSS. Each POSS molecule has two PEPI groups.



Scheme 1: Synthesis of  $\text{Ph}_8\text{BisPEPI-POSS}$



Table 1. Thermal transition of different PEPI compounds investigated.

<b>Compound</b>	<b>Thermal Transition (°C)</b>	<b><math>\Delta H_m</math> (kJ/mol)</b>	<b><math>\Delta H_c/\Delta H_m</math></b>
Ibu <sub>7</sub> propylPEPI-POSS	T <sub>m</sub> =157; T <sub>c</sub> =87	35.4 ± 2.0	0.608
Ibu <sub>7</sub> phenylPEPI-POSS	T <sub>m</sub> =238; T <sub>c</sub> =178	46.5 ± 1.0	0.855
Ph <sub>7</sub> phenylPEPI-POSS	No thermal transitions observed prior to PEPI reaction.		
Ibu <sub>7</sub> diPEPI-POSS	T <sub>m</sub> =190; T <sub>c</sub> =120	57.4 ± 6.4	0.364
Ph <sub>7</sub> diPEPI-POSS	T <sub>m</sub> =296	40.9 ± 0.9	N/O
Ph <sub>8</sub> bisPEPI-POSS	T <sub>g</sub> =100		
HFPE-n-9	T <sub>g</sub> =249		
HFPE-n-1	T <sub>m</sub> =340		
OctapropylPEPI-POSS	T <sub>m</sub> =234; T <sub>c</sub> =190	160 ± 4.7	0.831
OctaphenylPEPI-POSS	T <sub>g</sub> =205		

[note: Thermal transition is either the first order melt transition, T<sub>m</sub>, or the second order glass transition, T<sub>g</sub>. For first order transition, the corresponding heat of fusion,  $\Delta H_m$ , was determined from the area of the melting peak and normalized with respect to the molar weight of specific compound. Fraction of crystallization upon cooling was determined from the ratio of heat of crystallization from the cooling curve over the heat of fusion in heating,  $\Delta H_c/\Delta H_m$ . Thermal transitions were determined by a DSC with heating and cooling rate of 20°C per minute.]

Table 2. Results of the n<sup>th</sup> order reaction kinetics model analysis.

Temp. (°C)	<u>Ibu<sub>7</sub>propyl</u> k(min <sup>-1</sup> ) n	<u>Ibu<sub>7</sub>phenyl</u> k(min <sup>-1</sup> ) n	<u>Ph<sub>7</sub>phenyl</u> k(min <sup>-1</sup> ) n	<u>Ibu<sub>7</sub>di</u> k(min <sup>-1</sup> ) n	<u>Ph<sub>7</sub>di</u> k(min <sup>-1</sup> ) n	<u>Ph<sub>8</sub>bis</u> k(min <sup>-1</sup> ) n	<u>Octapropyl</u> k(min <sup>-1</sup> ) n	<u>Octaphenyl</u> k(min <sup>-1</sup> ) n	<u>HFPE-n-9</u> k(min <sup>-1</sup> ) n
340		0.869 1.154		1.403 1.863	0.706 1.479	1.528 1.951	1.751 1.592	1.055 1.439	
350	1.086 1.251	1.249 1.023		1.903 1.554	1.116 1.368	2.661 1.927	2.341 1.281	1.325 1.219	
360	1.668 1.176	1.917 0.945	0.141 0.633	2.686 1.354	1.790 1.291	3.926 1.818	3.269 0.995	1.637 0.984	1.029 1.655
370	2.472 1.098	2.017 0.905	0.360 0.631	3.941 1.175	2.916 1.285	5.445 1.550	4.890 0.769	2.047 0.744	1.761 1.623
380	3.620 0.999	4.670 0.879	0.708 0.603	6.135 1.077	4.446 1.235	8.023 1.390	8.055 0.608	2.887 0.611	2.564 1.294
390	5.334 0.893	7.187 0.854	1.288 0.552	9.740 0.963	6.753 1.184	11.741 1.231	14.920 0.503	4.514 0.517	4.070 1.084
400	8.131 0.767	10.837 0.807	2.390 0.489	16.576 0.847	10.329 1.166				6.772 0.956
410	13.200 0.651	15.960 0.754	4.841 0.434						12.042 0.872

[Note: Reaction rate constant, k (min<sup>-1</sup>) of phenylethynyl and order of reaction, n, at different temperatures for various PEPI-POSS molecules. Analysis was performed using dynamic heating curves at four different heating rates as obtained by DSC.]

Table 3. Characteristics of phenylethynyl reaction profiles.

<b>Compound</b>	<b>T<sub>Rxn, max</sub> @ 2, 5, 10, 20°C/min rate</b>	<b>ΔH<sub>Rxn</sub> (kJ/mol)</b>	<b>ΔH<sub>partial</sub> /ΔH<sub>total</sub></b>	<b>Activation Energy (kJ/mol)</b>
Ibu <sub>7</sub> propylPEPI- POSS	355.8, 375.0, 392.1, 410.0	176 ± 9	51 ± 3	140
Ibu <sub>7</sub> phenylPEPI- POSS	359.5, 377.5, 391.3, 409.6	175 ± 11	60 ± 2	155
Ph <sub>7</sub> phenylPEPI- POSS	382.4, 400.0, 405.9, 420.2	107 ± 35	52 ± 3	203
Ibu <sub>7</sub> diPEPI- POSS	349.3, 368.2, 384.3, 400.4	163 ± 16	54 ± 2	146
Ph <sub>7</sub> diPEPI- POSS	361.3, 378.8, 394.2, 413.7	84 ± 1	58 ± 2	149
Ph <sub>8</sub> bisPEPI- POSS	343.1, 359.6, 375.6, 395.0	134 ± 13	49 ± 2	141
OctapropylPEPI- POSS	331.0, 349.3, 367.4, 382.6	143 ± 7	41 ± 4	143
OctaphenylPEPI- POSS (LTP)	326.0, 349.6, 362.0, 373.9	95 ± 7	22 ± 3	143
OctaphenylPEPI- POSS (HTP)	352.5, 372.9, 391.0, 407.3	95 ± 7	49 ± 5	137
HFPE-n-9	365.2, 385.1, 396.3, 410.7	140 ± 24	47 ± 2	175
HFPE-n-1	363.1, 382.0, 394.4, 415.3	131 ± 3		152

[Note: T<sub>Rxn, max</sub> is the reaction peak maximum temperatures at the specified heating rate; ΔH<sub>Rxn</sub> is the average heat of reaction per mole of PEPI and its range from four different heat rates used; ΔH<sub>partial</sub>/ΔH<sub>total</sub> and Activation energy are the extent of reaction and energy barrier of reaction at T<sub>Rxn, max</sub>, respectively.]